LUND
UNIVERSITY

Aerodynamic Design in Axial Turbine for Heavy Duty Applications

Eric Lennman

Thesis for the degree of Master of Science in Engineering

Lund University | Faculty of Engineering | Department of Energy Sciences

Aerodynamic Design in Axial Turbine for Heavy Duty Applications

by Eric Lennman

LUND
UNIVERSITY

Thesis for the degree of Master of Science
Thesis advisors: Prof. Magnus Genrup, Dr. Per Andersson and Dr. Ulf Aronsson

To be presented, with the permission of the Faculty of Engineering of Lund University, for public criticism on the online meeting at the Department of Energy Sciences on Thursday, the 11th of June 2020 at 09:00.

This degree project for the degree of Master of Science in Engineering has been conducted at the Division of Thermal Power Engineering, Department of Energy Sciences, Faculty of Engineering, Lund University.

Supervisor at the Division of Thermal Power Engineering was Professor Magnus Genrup
Supervisor at Volvo Powertrain Engineering was Dr. Per Andersson and Dr. Ulf Aronsson

Examiner at Lund University was Associate professor Marcus Thern

The project was carried out in cooperation with the R&D department at Volvo Powertrain Engineering, Malmö.

Department of Energy Sciences
Faculty of Engineering
Lund University

ISSN: <0282-1990>
LUTMDN/TMHP-20/5456-SE

Typeset in LaTeX
Lund 2020

Contents

List of Figures

List of Tables

Nomenclature

Roman Letters

a	Speed of sound	$[m/s]$
A	Area	$[m^2]$
c	Blade chord	$[m]$
C	Absolute velocity	$[m/s]$
C_m	Axial velocity	$[m/s]$
C_L	Lift coefficient	[-]
C_p	Specific heat capacity at constant pressure	$[J/kgK]$
C_v	Specific heat capacity at constant volume	J/kgK
F	Force	$[N]$
g	Gravitational constant	$[m/s^2]$
h	Specific enthalpy	$[J/kg]$
i	Incidence angle	[-]
K_s	Loading factor	[-]
$\dot{m}$	Mass flow	$[kg/s]$
M	Mach number	[-]
P	Total Pressure	$[Pa]$
r	Radius	$[m]$
R	Specific gas constant	$[J/(molK)]$

s	Blade pitch	$[m]$
S	Body force	$[F]$
T	Total Temperature	$[K]$
U	Rotational velocity	$[m/s]$
v	Velocity	$[m/s]$
V	Volume	$[m^3]$
W	Relative velocity	$[m/s]$
$\dot{W}$	Power	$[W]$
Z	Loading factor	[-]
u, v, w	Velocity components	$[m/s]$
x, y, z	Cartesian coordinates	

Greek Letters

α	Absolute flow angle	[-]
β	Relative flow angle	[-]
γ	Specific heat ratio	[-]
δ	Deviation angle	[-]
ϵ	Hade angle	[-]
η	Efficiency	[-]
Λ	Enthalpy	[-]
μ	Dynamic viscosity	$[kg/ms]$
ξ	Vorticity	[-]
ρ	Density	$[kg/m^3]$
σ	Stress	$[N/m^2]$

τ	Torque	$[Nm]$
ϕ	Flow coefficient, tangential coordinate	[-]
ψ	Stage Loading	[-]
ω	Angular velocity	$[rad/s]$

Abbreviations

BMEP	Brake mean effective pressure	$[Pa]$
BSFC	Brake specific fuel consumption	$[g/Wh]$
CFD	Computational Fluid Dynamics	
GTT	Group Truck Technology	
LE	Leading edge	
PE	Powertrain Engineering	
PR	Pressure ratio	[-]
TE	Trailing edge	

Subscripts

0	Static
1	Inlet
2,3	Outlet
h	Hub
s	Isentropic
ts	Total to static
tt	Total to total
tq	Torque based
θ	Tangential component

Sammanfattning

Design inom turbomaskiner baseras på flertaliga förhållanden inom termodynamik och fluidmekanik. Mjukvara som implementerar dessa förhållanden genom flödesberäkningar har varit väl tillgängligt för allmänheten sedan 1990-talet och de har även blivit mera applicerade mot turbindesign. Denna mjukvara är dessvärre ofta en kapitalintensiv del inom avdelningar inom forskning och utveckling. Professor Emeritus från Cambridge Universitet John D. Denton släppte sitt eget-utvecklade program för turbindesign och flödesberäkningsprogram MULTALL år 2017 fritt för allmänheten. Detta program har undersökts i denna rapport om det är ett lämpligt verktyg för att ersätta ett existerande designverktyg. För detta arbete har programmet applicerats mot en en-stegs axial turbocompound-turbin som används i tyngre lastbilar. Målet var att både undersöka programmets designförfarande in och utvärdera dess prestanda mot en befintlig turbin som mall. En parameterstudie har gjorts för en möjlig elektrisk turbocompound-turbin och två turbindesigner för en elektrisk turbocompound-turbin har byggts. En implementering av elektrisk turbocompound-turbin förbättrar den övergripande verkningsgraden när rotationshastigheten för turbocompound-turbinen kan fritt väljas. Dessa beräkningar i MULTALL har validerats mot beräkningsprogrammet STAR-CCM+ och resultatet som erhölls i MULTALL har varit mycket nära resultatet från STAR-CCM+. Jämförelsen i prestandan mot turbinmallen var i storleksordningen 1 procentenhet.

Abstract

Turbomachinery design is based on multiple physical thermodynamical relations and fluid mechanics. Software implementing these relations in computing fluid flows have been broadly accessible since the 1990's and has also become more applied to turbomachinery design. However, the software is unfortunately a large expense on research and development departments. Cambridge Professor Emeritus John D. Denton released his self developed turbomachinery design software and computational fluid dynamics (CFD) solver, MULTALL, in 2017 making it freely accessible to the public and this software has been examined if it is a suitable tool for replacing an existing design tool. The software is has in this thesis been applied to a single stage axial turbo compound turbine used in heavy duty trucks. The goal was to both examine the design procedure in the software and evaluate the performance by comparing it to an existing base design. A parameter study for a possible electrical turbo compound unit was made and two designs for an electrical turbo compound application was made. The implementation of and electric turbo compound unit increases the overall efficiency as the turbo compound turbine can freely choose the revolution speed. The calculations obtained in the software has been validated through CFD software STAR-CCM+ and the performance obtained in MULTALL has been very accurate compared to results from STAR-CCM+. The performance comparison to the base turbine design has been in the order of 1% point as difference.

Chapter 1.

Introduction

Since the invention of the wheel, humans have used the fundamentals of energy that the wheel enable its user: the transfer of energy through motion. As the early wheels only used limited forces such as gravity or human force to roll, the invention of internal combustion engines facilitated an excellent way of transportation. Engineers have, through the development of vehicles, wanted to refine the engine terms of reliability and to produce more power. Since the oil crisis in the 1970's the fuel consumption has become more important and with the findings of the greenhouse effect, the fuel consumption has become even more crucial. With more efforts to decrease the emissions in every part of human activity, the transportation industry is set to decrease the carbon emissions with 15% by 2025 and 30% by 2030 [1]. An attempt to look into new design tools and configuration in one part of the exhaust heat recovery system at Volvo PE Malmö was performed for this thesis.

1.1. Background

Volvo Group manufactures trucks, buses, marine and industrial engines and construction equipment. Volvo Group Truck Technology (Volvo GTT) is a business area within Volvo Group that is dedicated to research and development towards the trucks in Volvo Group. The facility in Malmö (Volvo PE Malmö) develops components such as turbochargers, turbo compound units and component setups designated to heavy duty trucks. Volvo PE Malmö also validates new designs and concepts in their test riggs.

A turbocharger consists of a turbine and a compressor, see 3 and 2 respectively in figure 1.1. When the engine combusts air and fuel, the exhaust gases leaves the engine with high kinetic energy and potential energy from the pressure difference over the turbine and enter the turbine, making it spin. The turbine extracts kinetic energy from the working fluid and power is generated. The turbine is directly linked to the compressor through a shaft and the work from the turbine is transferred to the compressor. The compressor receives air from the intake, compresses the air and delivers it to the combustion chamber with air. The air can now combust with more fuel and the work output is increased compared to a

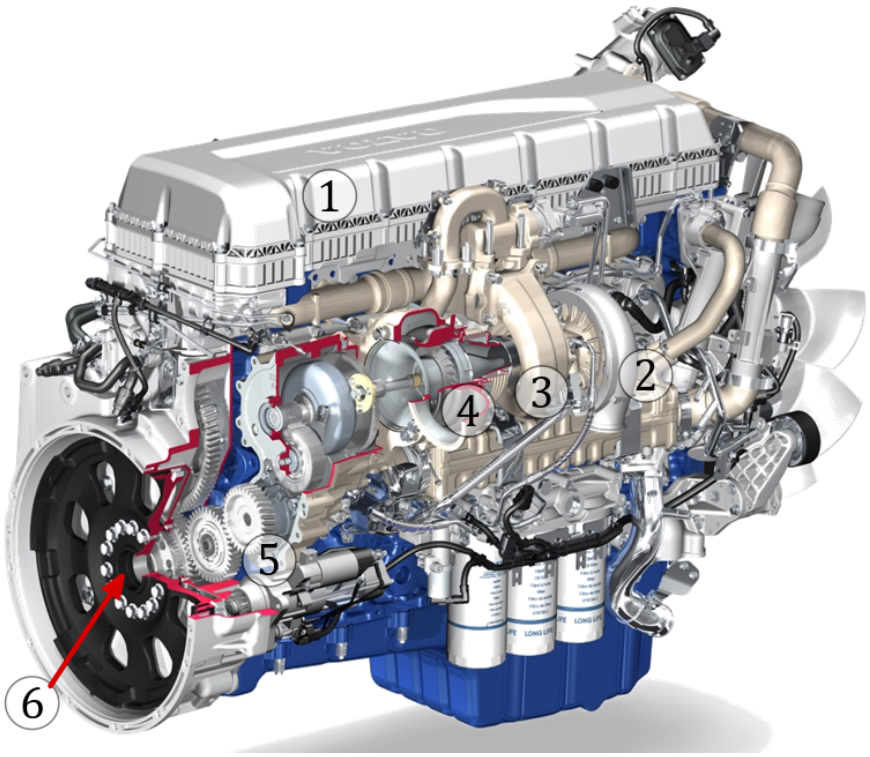

Figure 1.1.: VOLVO D13 engine (courtesy of Volvo GTT) 1: Internal combustion engine, 2: Compressor, 3: Turbine, 4: Turbo compound unit, 5: Couplings, 6: Crankshaft

naturally aspirated (i.e non-turbocharged) combustion engine. A turbocharger comes in different forms and depending of the application, different types of turbomachines are used. The engine studied in this thesis uses a turbocharger together with a turbo compound turbine which is a second turbine that extracts energy from the exhaust gases after the turbocharger turbine and transmits the torque directly to the engine crankshaft, see 4, 5 and 6 in figure 1.1.

1.2. Objective

The turbo compound turbines (TC turbine henceforth) needs to operate with a broad span of considerably high and low rotational speeds and the TC turbine is therefore subject to broad ranges in working conditions. From this, the turbine design is a great compromise in aerodynamics, structural integrity, size, etc. With new emission regulations coming into force by 2025, many parts in the waste heat recovery will be more important to reach the required CO2 reduction. exhaust heat recovery must improve and the TC turbine is therefore under scrutiny. Design in turbomachinery are constantly improving from new designing methods, tools and scientific findings. Design and computating tools carries a heavy cost on many research and development departments for every industry.

With the spreading and sharing of knowledge through open-source projects there are today new, freely available software such as GNU Octave, Psilab and Anaconda as substitutes to other expensive software. In the year of 2017 Cambridge professor in turbomachinery John D. Denton released his self-developed designing tool for turbomachinery to the public — MEANGEN, STAGEN and MULTALL. The software includes both a preliminary mean-line design, blade generation and a full 3D-simulation software. It is of great interest to investigate whether this design tool is a valid option to use for preliminary design at Volvo GTT.

The goal is to apply the design tool to a base setup of a TC unit at Volvo GTT. Together with the new design tool, new configurations as electrifying the TC unit and working conditions of the TC turbine is to be investigated. With an electric TC (E-TC) turbine the rotational speed can be set independently of the engine which gives less off-design operation compared to a mechanically coupled TC turbine. In addition, the work is carried out with an ambition of improving the peak efficiency and also improve the overall efficiency.

Learning a new design software can often be a frustrating task with many new design philosophies to learn and therefore the theory section of this thesis will cover the fundamentals in turbomachinery design. The end result is to apply the new design tool to the application of a E-TC unit and to reflect over the aerodynamical influence of the use of a E-TC.

1.3. Constraints

When designing a turbine there are many more aspects to account for than just aerodynamics, such as structural integrity, thermal loads, etc. This thesis will be constrained to focus more on the methodology of designing a turbo compound turbine and the aerodynamic aspects in the design. The turbine will only be considered as a standalone unit and the thermal interaction with the environment (engine, exhaust system, etc.) will therefore not be considered. The structural integrity of the new designs will only be described in short and no FEM will be performed. Some CFD implementation and its effects on the result will be discussed but to a minimum extent.

Chapter 2.

Theory

This section addresses the applicable theory to the goals of this thesis. Turbomachinery in vehicle applications treats both fundamental thermodynamics for extracting work from the fluid but also specialized knowledge in aerodynamics and loss modelling.

Turbomachines are divided in turbines and compressors in which turbines extract energy from the working fluid and a compressor transfers energy to the working fluid. The compressor can be divided into multiple devices such as blowers, pumps or fans. The extraction or addition of energy to the working fluid is different as a process but the principles for the practice are the same. A turbomachine in its simplest form consists of a stationary blade and a rotating blade, henceforth denoted as stator and rotor respectively. A radial turbine can consist of only a rotor. This set of a stator and rotor is called a stage and a turbomachine can consist of multiple stages depending on the application of the turbine. Turbines and compressors can take different shapes and forms but they are mostly divided into radial, axial or mixed flow. Since this master thesis focuses on axial turbines, the configuration of interest is therefore in axial flow turbines. In the axial turbine the stator and rotor are positioned circumferential to the flow. The stator leads the flow in a suitable direction so the fluid flows to the rotor and turns the blade to rotation, thus extracting work. The rotor is connected to a shaft that can be connected to a generator to produce electric energy [2].

2.1. Fundamental Thermodynamics

There are rigorous proof and demonstrations of how the laws of thermodynamics is applied to turbomachinery such as performed by Cengel and Boles [3]. This thesis is directed towards graduate students at any engineering faculty of relevance and the derivations are therefore deemed needles and will not be derived in this thesis. Instead the reader can be satisfied by the fruit of their labour. The energy conservation equation states that the sum of energy that flows through the boundary of an open control volume must equal zero. The energy equation is described in equation (2.1)

$$\dot{Q} - \dot{W} = \dot{m}[(h_2 - h_1) + \frac{1}{2}(C_2^2 - C_1^2) + g(z_2 - z_1)] \tag{2.1}$$

The specific enthalpy h and specific kinetic energy $\frac{1}{2}c^2$ is defined as the stagnation enthalpy, h_0

$$h_0 = h + \frac{1}{2}C^2 \tag{2.2}$$

Equation (2.1) can be manipulated further into something more convenient. The turbine used in a truck is positioned with a horizontal flow through the turbine and the change in potential energy can therefore be neglected. In an incompressible flow, the density of the fluid is constant. Combining equation (2.2) with equation (2.1) gives the energy equation as equation (2.3)

$$\dot{Q} - \dot{W} = \dot{m}(h_{02} - h_{01}) \tag{2.3}$$

The speed of the fluid through a turbine is commonly very large and with turbines having a fluid travelling faster than the speed of sound through the compressor. It is therefore convenient to introduce a relation between the fluid speed and the speed of sound. The Mach number is defined as following

$$M = \frac{v}{a} \tag{2.4}$$

With v as the fluid speed and a is the speed of sound, which is defined by the specific heat ratio, γ, the fluid temperature T and the gas constant R:

$$a = \sqrt{\gamma RT} \tag{2.5}$$

The density varies with the velocity of the fluid. The density change is about 5% when $M = 0.3$ and the transition from incompressible to compressible is considered to occur at $M = 0.3$ [4].

2.1.1. Gas Properties

In the previous section, the properties of the gas was not fully asessed and how the fluid is going from state 1 to 2 was not relevant. However the pressure, temperature and density will vary through the turbine and so will the gas properties. It is therefore of great interest to describe the behaviour of the gases. It is important to differentiate what kind of gas is used in a turbine and the most common gases are steam, exhaust gases

and air. With exhaust gases being used in this particular application, the theory will be restricted to the concepts of ideal and perfect gases.

An ideal gas follows the ideal gas relationship

$$pV = nRT \tag{2.6}$$

With R being the specific gas constant for every ideal gas at $R = 8.314\,J/(molK)$. m is the mass of the fluid, p is the pressure and V is the volume of the gas. The gas constant is defined by equation (2.7)

$$R = C_p - C_v \tag{2.7}$$

Where C_p is the specific heat at constant pressure and C_v is the specific heat at constant volume.

$$C_p = \left(\frac{\partial h}{\partial T}\right)_p \tag{2.8}$$

$$C_v = \left(\frac{\partial h}{\partial T}\right)_v \tag{2.9}$$

In MULTALL's solution manual C_p is set to vary quadratically with temperature:

$$C_p = C_{p1} + C_{p2}(T - T_{ref}) + C_{p3}(T - T_{ref})^2 \tag{2.10}$$

2.2. Turbomachinery

In this section we will lay out the theory that is used in turbomachinery. Firstly we need to define the coordinate system that is used. It is most suitable to leave the carteesian coordinate system and instead utilize the cylindrical coordinate system (r, ϕ, z) which is the radius, tangential angle and axial coordinates in that order. Besides the cylindrical coordinate system we introduce the meridional view which is what the reader can see in figure 2.1.

2.2.1. Blade Profile

A blade profile can be represented in several ways. The development of blade profiles started in 1884 as Horatio F. Phillips patented the first airfoils, which was applied to aircrafts. However, the blade nomenclature are the same in turbomachinery. In the early 1900s the National Advisory Committee for Aeronautics (NACA) performed a

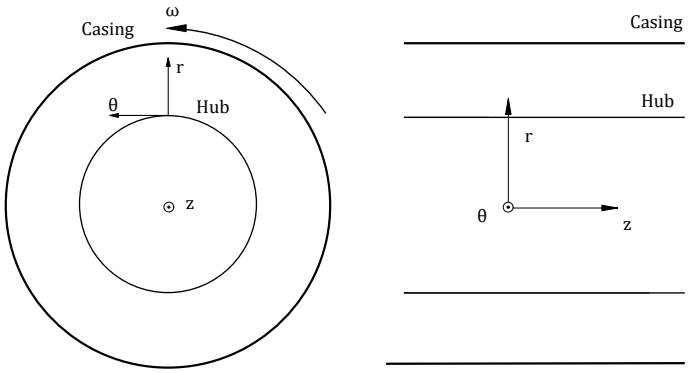

Figure 2.1.: Cylindrical coordinates r, ϕ, z and the meridional view (right)

standardised designing method by defining the logical numbering system by varying the chord, the location of maximum camber in relation to the chord length and maximum thickness in relation to the chord length [4]. This was further developed with more parameters. In turbine design the most typical blade section parameters are shown below.

The front and back end of the blade are called trailing and leading edge respectively (LE and TE henceforth in this thesis). The root, or the hub, is the radial section nearest the shaft or axis of rotation, and the shroud, or the tip, is the radial section most farthest away from the shaft. With a turbomachine that consists of multiple blade profiles in a sequence we need to put the blades in relationship to eachother. The minimum distance between the blades, the throat A, is important to define when the designer want to choke the flow. The spacing, or pitch, is denoted as s which is also important to assertain a proper turning of the flow. The deviation angle, δ, is the difference of the exit blade angle and the angle of the fluid leaving the cascade. As the deviation relates the real and blade outlet angle the incidence angle, i, is the difference between inlet fluid angle and the inlet blade angle.

2.2.2. Fluid Flow

When the fluid enters the turbine stage, the fluid will attach to the leading edge of the blade and leave the blade at trailing edge. With a stator as the first blade the fluid velocity is easy to understand relative to the stationary part but when the fluid enters the rotating blade the fluid velocity must be divided into a relative velocity and actual velocity. It is therefore convenient to divide the real velocity, C into two parts.

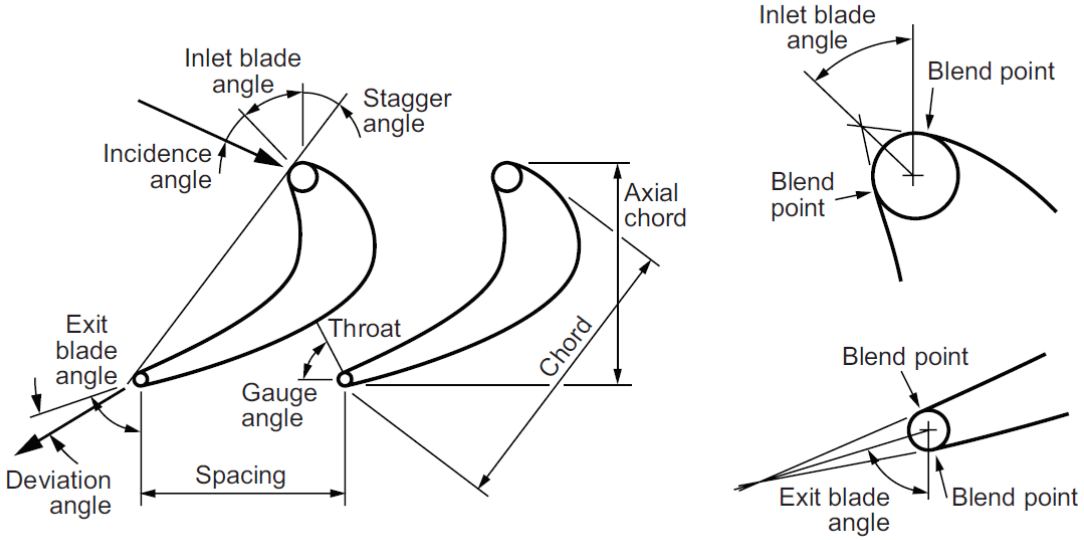

Figure 2.2.: Turbine blade parameters [5]

$$\mathbf{C} = \mathbf{W} + \mathbf{U} \tag{2.11}$$

The absolute velocity, C is the vector sum of the relative velocity W and the rotational velocity U. Equation (2.11) is denoted in vector form since it can be used in the cylindrical space in the turbine. For a radial section of a single stage turbine velocities can be described in figure 2.3.

The angle α between the axial velocity C_m and the absolute velocity C is called the absolute flow angle and β is the relative flow angle. One should be cautious with the indices of the velocity triangles at figure 2.3. Since the flow in the TC turbine is completely axial there is no angular component in the inlet velocity triangle, meaning that $C = C_m$. The indices goes otherwise (when there is an inlet angular component) as 1 being the stage inlet, 2 as rotor inlet and 3 as stage outlet. Other equations in this stage regarding the whole turbine uses index 1 as inlet and 2 as the outlet. The velocity components are following:

$$C_m = C \cos \alpha \tag{2.12}$$
$$C_\theta = C \sin \alpha \tag{2.13}$$
$$W_m = W \cos \beta \tag{2.14}$$
$$W_\theta = W \sin \alpha \tag{2.15}$$

These equations are key components when designing a turbine, since the turbine is there

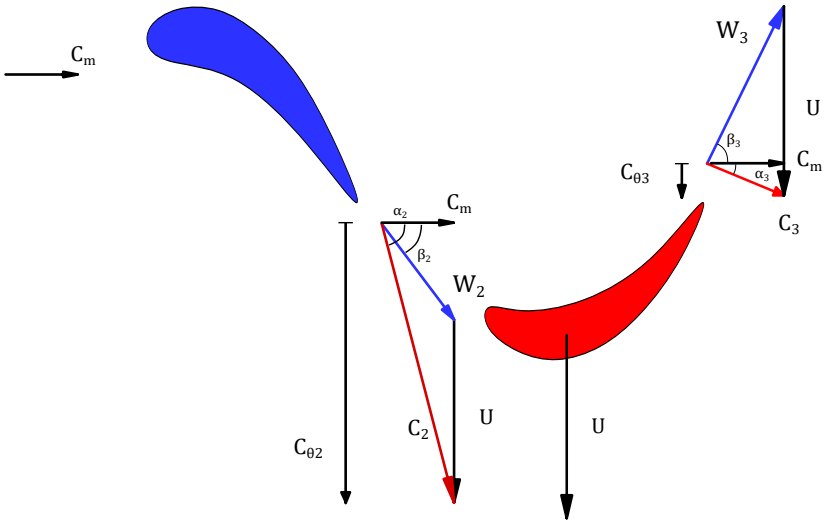

Figure 2.3.: Flow angles for a stage

to turn the flow and extracting work from the fluid. The turning of the flow and the work extraction was described by Leonhard Euler in the Euler turbine equation:

$$\dot{W}_t = \tau\omega = U_1 C_{\theta 1} - U_2 C_{\theta 2} = U(C_{\theta 1} - C_{\theta 2}) \tag{2.16}$$

Where index 1 is the turbine inlet and 2 is the turbine outlet. Equation (2.16) shows that the turbine work is done from the difference in tangential velocity C_θ. The aim as a turbine designer is therefore to maximize the amount of turning as efficiently as possible without creating too much loss.

2.2.3. Turbine Efficiency

In every occurrence of irreversible entropy creation in the turbine flow, there will be a decrease in used work, thus an efficiency decrease. The efficiency of a turbine can be described in multiple ways but the most common definitions will be described in this thesis. The isentropic efficiency is the fraction of actual work and the available work.

$$\eta = \frac{h_{01} - h_{02}}{h_{01} - h_{02,s}} \tag{2.17}$$

Where $h_{02,s}$ is the enthalpy obtained when expanding the fluid at constant entropy to state 2. The inlet or exit state may be considered as total or static and depending on the application of the turbine there may be of interest to clarify this. With an exit state where the kinetic energy is used there might be more relevant to include the total state in the efficiency. We can therefore introduce the total to total efficiency (tt) and total to static (ts) efficiency. The efficiencies are defined as follows:

$$\eta_{tt} = \frac{h_{01} - h_{02}}{h_{01} - h_{02,s}} \tag{2.18}$$

$$\eta_{ts} = \frac{h_{01} - h_{02}}{h_{01} - h_{2,s}} \tag{2.19}$$

In engine performance, it is interesting to see how the energy process in the turbine is transmitted to the shaft and a torque based efficiency is introduced. The torque that the turbine provides is denoted τ in Newton meter, N is the rotational speed in revolutions per minute. The heat capacity ratio is denoted γ. The torque based efficiency can also be described in total to static terms which is considered a more reliable efficiency:

$$\eta_{tq,ts} = \frac{\tau N 2\pi/60}{\dot{m} c_p T_{01} \left(1 - \left(\frac{P_2}{P_{01}}\right)^{\frac{\gamma-1}{\gamma}}\right)} \tag{2.20}$$

2.2.4. Loss Mechanisms

As described earlier about efficiency; there will be an irreversible process and an increase in entropy will occur. The causes of the efficiency deterioration was not described earlier but is now dedicated the attention needed.
When modelling a turbine there are several aspects that affects the optimal flow through the turbine, i.e the efficiency. John D. Denton's report on loss mechanisms in turbomachinery [6] describes the division of losses into profile, endwall and leakage losses and its non-independence. His report is heavily cited by many studies and literature within turbomachinery and the reader is recommended to read this report for further information. Denton gives in his paper of loss mechanisms a fundamental understanding of the losses in terms of entropy increases and that paper will be used as a main source in this thesis. Losses can be described in many ways and the author of this thesis uses the most convenient way which is the use of entropy increase.
The entropy creation in a turbine can be illustrated through the enthalpy-entropy diagram, see figure 2.4

Where state 2s is the isentropic expansion from state 1 to 2. The mechanisms for the entropy creation is described in [6] as

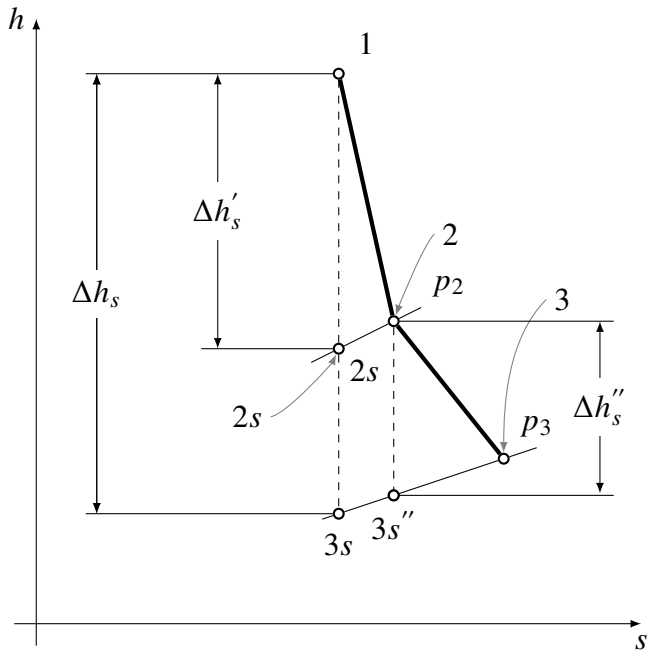

Figure 2.4.: Enthalpy-entropy diagram for the turbine expansion

- Viscous friction in boundary layers or free shear layers.
- Heat transfer across finite temperature differences.
- Non-equillibrium processes such as occur in very rapid expansions or in shock waves.

Secondary Flow

Secondary flow is the generation of loss that comes from turning of the flow and has some of its origin from endwall boundary layer. Sieverding [7] covers these effects in axial turbines from what was known at that time (1985). Dixon et. al [2] describes the secondary flows in terms of vorticity. Vorticity is a vector quantity with a direction along the axis of rotation. Consider an inlet flow to the stator in an axial turbine. The velocity profile of the flow is not uniform because of the friction losses between the fluid and the inner and outer wall. The vorticity ξ of this boundary layer is normal to velocity C

$$\xi_1 = \frac{\partial C_1}{\partial z} \tag{2.21}$$

With z being the distance from the wall. The direction of ξ_1 follows the right-hand screw rule. As the flow is guided to the pressure and suction side of the blade the vorticity is split into two vortices, see figure 2.5. The vortex on the pressure side will radially follow the suction side of the adjacent blade. The result is a highly rotational flow near the

suction side at hub and casing. When the flow leaves the stator blade the rotational flow will cause an overturn in flow at the pressure side and an overturn at the suction side due to the cross-passage pressure gradients.

This over- or underturning of the flow is one explanation for the deviation δ in figure 2.2.

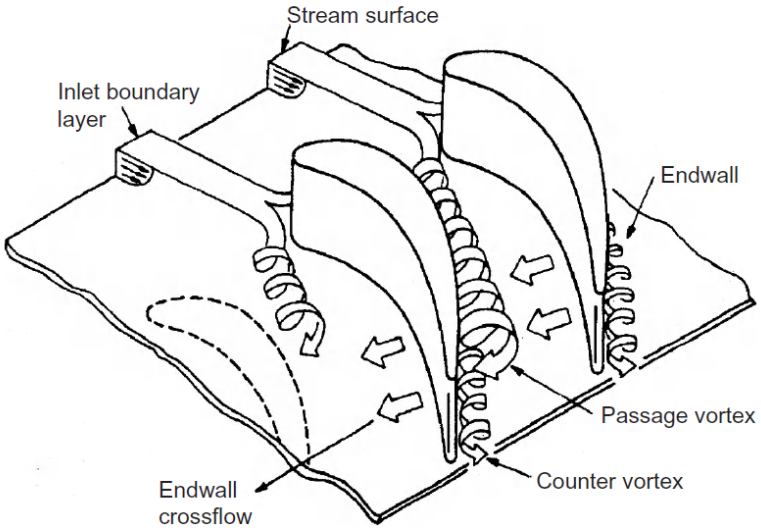

Figure 2.5.: Secondary flow within a blade passage [2]

These secondary losses must be accounted for and Baines [5] summarizes the key factors that should be considered when designing the turbine with secondary flow in mind:

As the secondary flows come from the turning of the blades, the *blade shape or blade loading* is one of the factors. At radial section the radius of curvature decreases with the deflection angle and the pressure gradient normal to the streamline increases, with too high pressure gradient separation will occur.

The solidity or the *pitch-chord ratio* affects the loading of the blade in similar sense as the blade shape. A too large pitch in relation to the chord gives less turning and a too large chord respectively chokes the flow too much and a optimum pitch-chord exists accordingly. The pitch-chord ratio s/c is simplified to:

$$Zw = 2\frac{s}{c}\cos^2\alpha_2(\tan\alpha_1 + \tan\alpha_2) \tag{2.22}$$

Where Zw is the Zweifel number which can range between $0.75 < Zw < 1.2$ depending on the flow case. For the TC turbine the Zweifel number is approximately 0.83. As the secondary flow losses occur mostly near the endwalls of the blade passage. The

ratio between the blade height and chord or *aspect ratio* and a high aspect ratio would therefore lower the effects of secondary losses.

An increase in *Mach number* is shown to be a good way to decrease the secondary losses as the boundary layer growth from which the secondary flow form.

Ainley-Mathieson Method

Ainley and Mathieson [8] formulated and represented the secondary losses by a loading factor Z

$$Z = \left(\frac{C_L}{s/c}\right)^2 \frac{\cos^2 \alpha_2}{\cos^3 \overline{\alpha}_3} \tag{2.23}$$

Where $\overline{\alpha}_3$ is an average passage flow angle:

$$\tan \overline{\alpha} = \frac{1}{2}(\tan \alpha_1 + \tan \alpha_2) \tag{2.24}$$

The lift coefficient $C_L$is approximated as (given for constant axial velocity and constant radius):

$$\frac{C_L}{s/c} = 2 \mid \tan \alpha_1 - \tan \alpha_2 \mid \cos \overline{\alpha} \tag{2.25}$$

The result from this was further developed by Dunham and Came (1970) which includes the blade aspect ratio (c/b) and the boundary layer thickness δ^* [5]

$$K_s = \left(\frac{c}{b}\right) Z \frac{\cos \alpha_1}{\cos \alpha_{2b}} f\left(\frac{\delta^*}{c}\right) \tag{2.26}$$

Further correlations have been developed and corrected through more cascade data and corrections thereafter and the reader can study this more in depth in literature from Dixon [2], Baines [5] or Saravanmutto et. al. [9]. However this thesis will rather stress that physical properties such as solidity and aspect ratio and their effects on the efficiency.

Tip Gap Losses

Tip gap losses are those losses that are related to the nonturning of flow by escaping through the gap between the blade tip and the turbine housing. With a freely rotating blade section the blade must be mounted so that the blade does not collide with the

housing. This can be solved by mounting the blade together with a shroud that prevents any clearance between the tip of the blade and the wall. This reduces the tip gap losses but increases manufacturing costs and the demand for structural integrity. The flow caused by tip gap losses can be illustrated through figure 2.6.

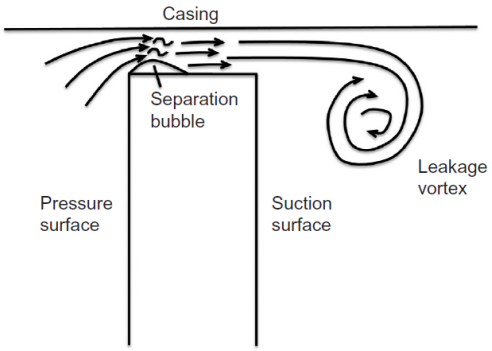

Figure 2.6.: Schematic of tip leakage flow [2]

An increase in tip clearance deteriorates the performance of the turbine as shown by [10], [11]. The driving forces of the clearance losses comes from the pressure difference between the suction and pressure side of the blade [10]. With a higher pressure difference between the pressure and suction side a higher amount of air will travel through the clearance instead. The tip gap losses can of course be reduced by a decrease in clearance, however this is only possible to a certain degree if the turbine should avoid to collide with the turbine housing if some mechanical vibration would occur. The losses can instead be reduced by decreasing the pressure difference between pressure and suction side, or in other terms reduce the tip reaction.

Trailing Edge Losses

When the fluids leave the blade a deviation always occurs in the outlet angles from the metal angle, the causes from this is described in the section about secondary flow. The entropy generated after the trailing edge is in the order of 15% of the total entropy increase [6]. As the flow detaches from the blade, the trailing edge shape can determine how well the flow is detached. A sudden sharp edge as trailing edge is not suitable as it produces large wakes behind the blade, leading to an increase in entropy. Both manufacturing aspects and aerodynamics say that an elliptical blade shape is preferable.

2.2.5. Performance Parameters

When designing a turbine there is a need for manipulating the turning of the flow and therefore adjust the velocity triangles. This can be done by further manipulation of the

relationships of the flow angles and the work output. Some new parameters such as reaction, loading coefficient and flow coefficient will be introduced in this section. These parameters are only in the one-dimensional analysis of the turbine and therefore are made for a specific radial section. It is often made in the design stage through the midsection at half blade span. Several manipulations will performed through the assumption of constant axial velocity.

Reaction is a relationship of the enthalpy drop of the stator to the enthalpy drop throughout the stage. If the enthalpy drop only occur in the rotor, the reaction will be zero. Conventionally, turbines are either designed as zero reaction stages or 50% reaction stages. These two types of turbines come with different advantages and drawbacks and are therefore suitable for different applications. The TC turbine that this thesis covers is a 50% reaction stage. The reaction is defined as follows:

$$\Lambda = \frac{h_2 - h_3}{h_1 - h_3} \tag{2.27}$$

The reaction can also be defined through pressure drop:

$$\Lambda_p = \frac{p_2 - p_3}{p_1 - p_3} \tag{2.28}$$

However, this equation should not be mixed up with the enthalpy based reaction as the pressure based does not give the same values as the enthalpy based. The reaction that is calculated in MULTALL is enthalpy based.

A common assumption in turbine design theory is the use of assuming that the axial velocity is constant throughout the stage. Equation (2.2) gives.

$$\Lambda = 1 - \frac{h_1 - h_2}{h_{01} - h_{03}} \tag{2.29}$$

Since the stator does not provide any work, the stagnation enthalpy will therefore remain constant which gives:

$$h_1 - h_2 = h_{01} - h_{02} + \frac{1}{2}({C_2}^2 - {C_1}^2) = \frac{1}{2}{C_m}^2(\tan^2\alpha_2 - \tan^2\alpha_1) \tag{2.30}$$

Stage loading relates the stage enthalpy drop and the rotational speed and is defined as:

$$\psi = \frac{\Delta h_0}{U^2} \tag{2.31}$$

Stage loading together with Euler turbine equation can be rewritten in terms of velocities:

$$\psi = \frac{\Delta C_\theta}{U^2} \tag{2.32}$$

The flow coefficient is the ratio of the axial (or meridional) velocity and the blade speed:

$$\phi = \frac{C_m}{U} \tag{2.33}$$

Using the mass flow equation one can compute the flow coefficient as:

$$\phi = \frac{\dot{m}}{\rho A U} \tag{2.34}$$

Equation (2.30), (2.32) and (2.33) can be combined into:

$$\psi = 2(1 - \Lambda + \phi \tan \alpha_1) \tag{2.35}$$

This shows that the performance of the turbine, or the turning of the flow, can be described through the stage loading, reaction and flow coefficient. This provides sufficient information to completely determine the velocity triangles.

The relationship between stage reaction, stage loading, flow coefficient and efficiency is well documented. The most important aspects will be covered in this thesis, as these are well proven to be efficient ways of improving the turbines.

Smith Chart

The influence of the stage loading and flow coefficient was first documented by Smith et. al. [2] who gathered large amount of data of multiple gas turbines at Rolls-Royce. The result was a chart over the turbine stage loading vs the flow coefficient and their relationship to the isentropic efficiency. The result was from turbines with zero tip clearances and the smith chart would therefore be considered as a guide to how the turbine would behave if the flow angles were changed. If a stage loading is set to a specific value and one would like to decrease the flow coefficient, the efficiency could increase as an result depending on what value the stage loading is.

Looking at equation (2.32) one can see that a lower amount of turning gives a lower stage loading. With the Smith chart showing an efficiency increase as stage loading decreases with flow coefficient. However the position in the Smith chart gives some characteristics in blade shape and blade loading.

When designing for lower ϕ the turbine blade will be a taller blade as the channel surface area increases (thus reducing the axial velocity) and this comes with a higher aspect ratio

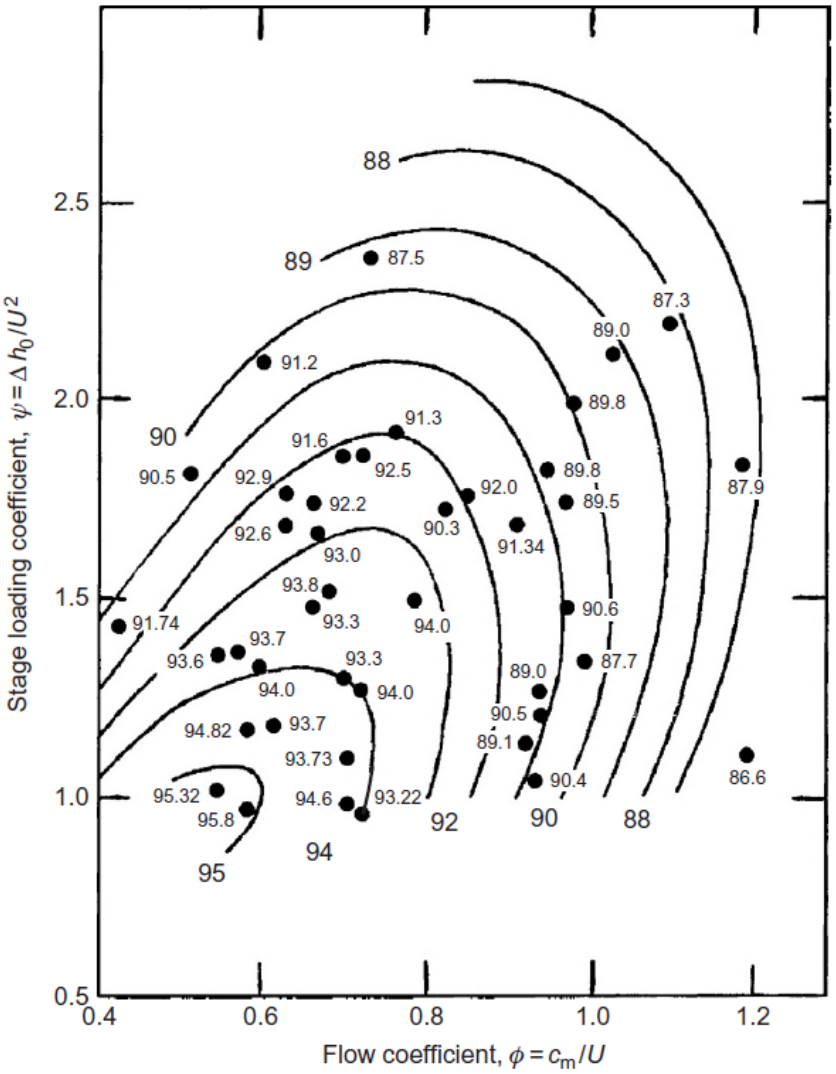

Figure 2.7.: Smith chart for turbine stage efficiency [2]

that lowers the secondary losses. A higher ϕ gives a shorter turbine blade as and aspect ratio which causes higher secondary losses. Turbines with low coefficient and stage loading gives in general terms higher efficiency as the blades suffers less from secondary losses. A higher flow coefficient generates a taller blade, which gives more wet surface and therefore higher secondary losses.

2.2.6. Blade Stacking

The blade profile and its effect on the aerodynamics have been explained earlier in this theory section but no address has been made to the three-dimensional blade shape.

The two-dimensional blade section covers many characteristics of the fluid flow and performance but how the sections are stacked is also important. By changing the blade stacking, the turbine designer can decrease tip clearances, change pressure distributions on the blade and these are discussed in this section.

The standard case where the blade sections are stacked radially and the sections can be stacked through simple lean, compound lean, and sweeping. There are other terms such as compound twist [12] but the ones most common used in STAGEN is simple lean and compound lean therefore described in this thesis.

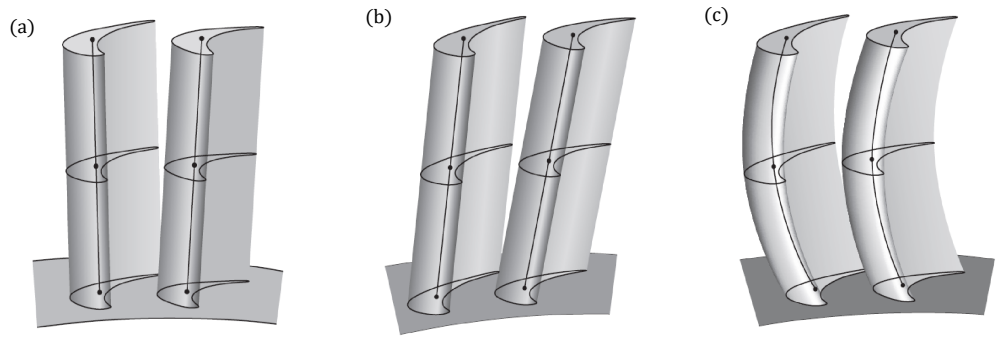

Figure 2.8.: Blade stacking with (a) radial stacking, (b) simple lean and (c) compound lean [5]

In the radial stacking case the isobars on the blade are almost perpendicular. If the blade is leaned, the blade applies a radial force and a radial pressure gradient is generated. Blade leaning shifts the pressure distribution on the blade and as described about tip gap losses, the losses from tip clearance can be reduced if the pressure difference between suction and static pressure side reduced.

Off-Design Performance

In the design process the stage loading and reaction is chosen for a specific radial section, i.e a 50% reaction stage is not necessarily 50% throughout the whole span. As the velocity triangles vary with the span so will the reaction, loading and flow coefficient. The turbine is seldom only operating in design load and therefore the off-design performance must be considered. As we will see in the following sections about turbo compounding a heavy-duty truck, the turbine will be governed by the engine and its temperature, pressure outlet, etc. This is combated by normalizing the speed to the inlet temperature and the derivation is performed in appendice. The normalized speed, N^* is defined as [9]:

$$N^* = \frac{N}{\sqrt{T_{01}}} \tag{2.36}$$

As the turbine must be operate in other conditions than the design case it is interesting to put N and T_{01} in relationship to the design case:

$$\frac{N/\sqrt{T_{01}}}{N_{des}/\sqrt{T_{01,des}}} \tag{2.37}$$

The actual flow case can now be represented as a fraction of the design case. This is useful to plot against the pressure ratio.

Similarly, a corrected mass flow $\dot{m}\sqrt{T_{01}}/P_{01}$ can be plotted against the pressure ratio. This is used to investigate the swallowing capacity of a turbine and comparison to other turbines can be made. The corrected mass flow is used as a representation of the swallowing capacity.

2.2.7. Stresses

The most dominant force on the turbine blades are the centrifugal forces from rotation. Pressure loading on the blade and thermal loading are also exerting forces on the blade but are not as large as the centrifugal loading and therefore not as important when reducing the stresses. As turbine blades can be stacked differently, the centrifugal forces will also change. Consider a simple radial stacked turbine blade. As the TC turbine is unshrouded, centrifugal stresses vary from zero at the tip to maximum at the hub. By integrating the blade mass and radius from hub to tip, you will obtain the hub centrifugal force, F_h:

$$F_h = \rho\omega^2 \int_{r_h}^{r_t} ar\,dr \tag{2.38}$$

where a is the area of the radial blade section, ρ is the density and ω is the angular speed. From the definition of stress as the force per unit of area gives further manipulations to (2.38). As the example is a simple radial stacked, the area is constant and the stresses become:

$$\sigma_h = \frac{F_h}{a_h} = \frac{\rho\omega^2}{a_h} \int_{r_h}^{r_t} a_h r\,dr = \frac{\rho\omega^2 A}{2\pi} \tag{2.39}$$

The conclusion is that the centrifugal stresses are proportional to the annulus area, A, and the rotational speed, ω or N squared. A compound lean often increases the stresses of the blade and this affect equation (2.39) but the relation $\sigma_h \propto AN^2$ is still important to consider.

2.3. Navier-Stokes Equations

The fluid flow and their properties have been discussed earlier in this thesis and it is now time to discover how to solve for fluid motions. In fluid dynamics one must consider what kind of fluid that is used (Newtonian, non-Newtonian fluid etc.) and if the fluid is compressible or incompressible. Air is considered as a Newtonian fluid and as the turbine operates in Mach numbers above 0.3 we solve this flow case by using the *Navier-Stokes equations* [13]:

$$\rho\frac{Du}{Dt} = -\frac{\partial p}{\partial x} + \text{div}(\mu \text{ grad } u) + S_{Mx} \tag{2.40}$$

$$\rho\frac{Dv}{Dt} = -\frac{\partial p}{\partial y} + \text{div}(\mu \text{ grad } v) + S_{My} \tag{2.41}$$

$$\rho\frac{Dw}{Dt} = -\frac{\partial p}{\partial z} + \text{div}(\mu \text{ grad } w) + S_{Mz} \tag{2.42}$$

These equations relates the three dimensional velocity u, v, w, the pressure p and the fluid dynamic viscosity μ to each other. In broader terms the equation can be broken down into intertial forces, pressure forces, viscous forces and external forces applied to the system in the order displayed in the equations (2.40)-(2.42). The Navier-Stokes equations are solved together with the continuity equation [13]:

$$\frac{\partial \rho}{\partial t} + \text{div}(\rho \mathbf{u}) = 0 \tag{2.43}$$

These equations are solved together with the boundary conditions such as walls, inlet and outlets and is performed iteratively. Solutions schemes used to reach convergence arer explained in the software instructions.

2.4. CFD

This section covers the solution schemes used in MULTALL and STAR-CCM+ and also some of the important physics models.

Multall uses the scree algorithm is an second order discretization method. The primary flow variable F ($F = \rho, \rho E, \rho V_x, \rho V_y$ or $\rho r V_t$) are for every timestep:

$$\Delta F = \left(2\left(\frac{\partial F}{\partial T}\right)^n - \left(\frac{\partial F}{\partial T}\right)^{n-1}\right)\Delta t \tag{2.44}$$

Where n is the time step level. In STAR-CCM+ a coupled flow can be used with a second order discretization. The coupled flow solves the conservation equations for mass, momentum and energy simultaneously using a pseudo-time-marching approach. This solving method is preferable when the fluid flow is a subsonic and compressible flow. In a turbomachine the flow is predominantly turbulent and so the behaviour of the fluid becomes more difficult to solve for. The Navier-Stokes equation governs the velocity and pressure of a flow as described in earlier section and each of these quantities can be separated into a mean part and a fluctuating part. The nonlinearity that comes from the turbulent flow becomes very difficult to calculate and so one must apply turbulence model to close the problem. MULTALL uses the Spalart-Allmaras turbulence model which solves a modelled transport equation for the kinematic eddy turbulent viscosity.

2.5. Turbo Compound Configuration and Performance

When fully understanding the concepts of turbomachinery outlined in this thesis it is then important to understand the application of the turbomachines, namely the turbo compound in this thesis and the engine performance. Some new physical properties will be therefore be outlined in this subsection together with the objectives of turbocharging an internal combustion engine, ICE.

2.5.1. Turbo Compound

The TC turbine was first applied to the aircraft industry with the Napier Nomad piston engine developed by Napier & Son in 1949 [14]. Further development in the aircraft industry made the turbo compound ICE less relevant from the competition of the turbojet and turboprop engine. The TC turbine found its renaissance in the 2000's as both Scania and Volvo implemented it [15] in their heavy duty trucks.

A TC turbine is a turbine that extracts energy from the working fluid in more than one stage. Turbines can be constructed with multiple stages whereas a TC turbine is a separate turbine that does not drive the compressor in the turbocharger. Figure 2.10 shows a drawing of how a typical TC-turbine is used together with a turbocharger setup. For a concept at Volvo GTT the TC-turbine is a single stage axial turbine which is linked through multiple gearings and a fluid coupling to the crankshaft of the engine, providing a transmission from the TC turbine to the wheels. A simple schematic of a TC setup is shown in figure 2.10:

The TC turbine is connected to the crankshaft of the engine through multiple gearings and a fluid coupling. The TC turbine co-revolves with the engine and adds torque from the work extraction in the TC turbine. This provides a great increase in power to the propulsion. Heavy duty trucks must operate at various combinations of vehicle speed

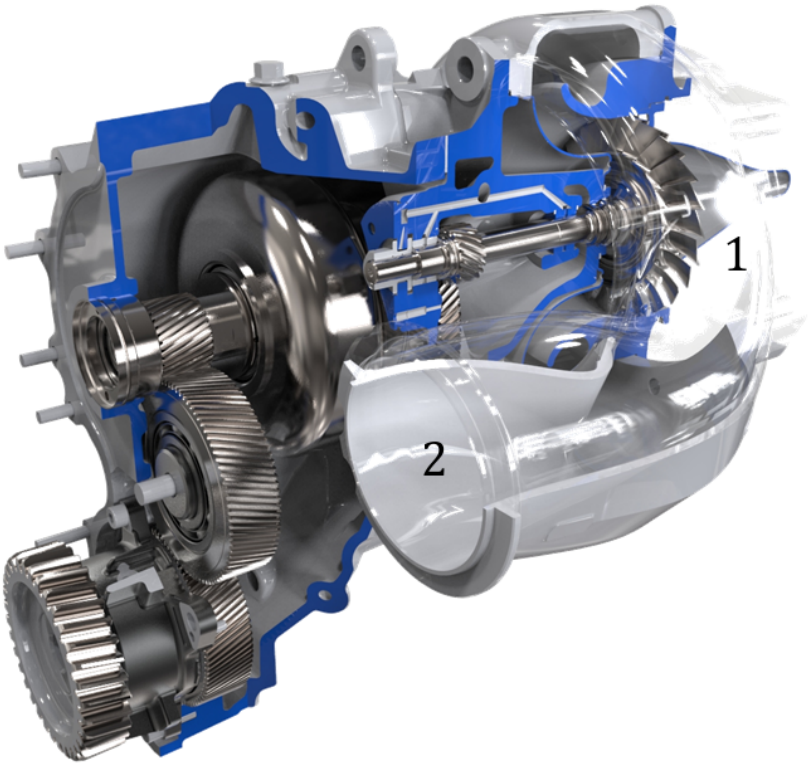

Figure 2.9.: Turbo compound unit with inlet (1) and exhaust (2) and the coupling to the crankshaft (courtesy of Volvo GTT)

and engine torque. Because of the direct coupling the TC turbine must also act in the same sense.

Multiple studies have shown an increase in overall efficiency of 4 - 7% when employing an electrical turbo compound unit [16], [17]. The TC turbine is decoupled from the crankshaft and drives a generator instead. The work from the TC turbine can be generated to electricity to power electrical components such as air-conditioning, ECUs, propulsion etc with propulsion being the most important use in heavy duty trucks applications. The electrical TC turbine will henceforth be called E-TC. The E-TC was introduced to formula 1 cars in 2013 to replace the propulsion from ICE in pit lane [18], allowing for hybrid concepts.

The E-TC is decoupled from the crankshaft making it revolve freely from the engine speed. As the performance of the turbine is greatly affected by the rotational speed, the E-TC can, with the use of a generator, regulate the rotational speed to a more suitable operating conditions. The E-TC can now find its "sweet spot" for every working condition.

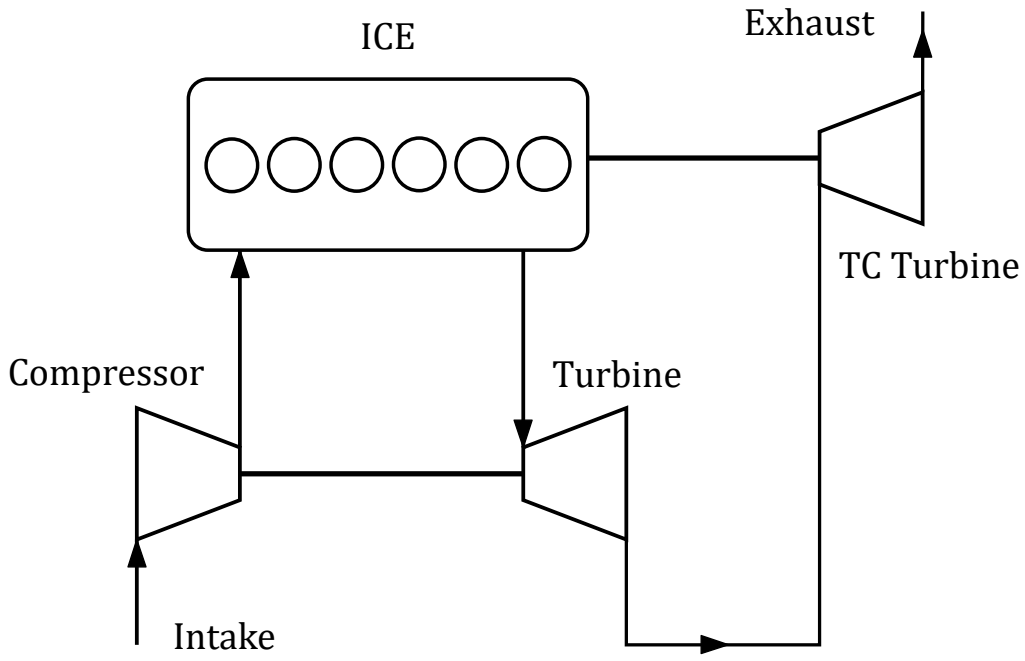

Figure 2.10.: Turbo compound setup

2.5.2. Heavy-Duty Trucks

When a vehicle manufacturer wants to specify how their engine performs they usually divide the performance of the product in many broad terms. It can be divided into economy, reliability and durability under service conditions to describe how the engine satisfies the needs of the customer. Additionally some technical specifications can be added to show more "hands-on" data of how the engine performs during use. A heavy-duty truck is expected to run in many different operating points such as high vehicle speed and low torque or vice versa. John B. Heywood [19] states the most important technical measures at the different operating points as:

1. At maximum or normal rated point:

   Mean piston speed

   Brake mean effective pressure (BMEP)

   Power per unit piston area

   Specific volume

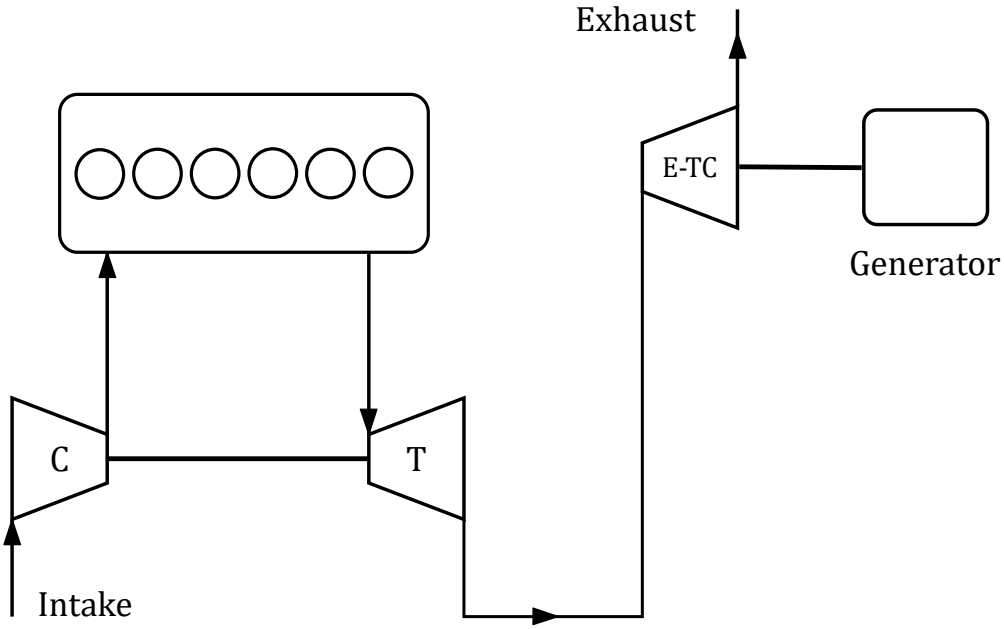

Figure 2.11.: New layout with the E-TC

2. At all speeds at which the engine will be used with full throttle or with maximum fuel-pump setting:

   BMEP

3. At all usefull regimes of operation and particularly in those regimes where the engine is run for long periods of time:

   Brake specific fuel consumption (BSFC)

   Brake specific emissions

In our scope it is most focus on the maximum power and torque and reducing the BSFC. In this thesis the goal is to replicate and improve a pre-designed TC turbine and to constrain the thesis in a manageable depth the results in operating conditions such as cycle analysis of the ICE is not performed.

Chapter 3.

Methodology

In this section we will describe the tools that was used for the results and an outline of the work flow is described. The program package from Denton is divided into three different scripts: MEANGEN, STAGEN and MULTALL. These programs will work as preliminary design of the axial turbine with some slight modifications depending of the application and demands from the operating points.

3.1. MEANGEN

MEANGEN is a mean-line turbomachinery design program. It uses input data from the users that defines the boundary conditions for the turbomachine such as inlet pressure, mass flow, inlet angels etc. With these basic design parameters it makes an initial guess of the blade shapes. MEANGEN is, like STAGEN and MULTALL, written in FORTRAN77 and the source code of MEANGEN was edited to obtain a design that would resemble the TC of today.

3.2. STAGEN

STAGEN uses the output data from MEANGEN as input and creates the final blade geometry which is then used in MULTALL. The blade geometry can be specified with tip clearances, bladings through Zweifel criterion etc.

To maintain a quick way of examining and judging the design the blade coordinates was extracted to GNU Octave. A script to illustrate the blade sections was obtained. If the design looked reasonable the work was then continued to MULTALL.

3.3. MULTALL

When the boundary conditions of the turbomachine is created and blade geometry is generated, the data is then used in MULTALL which is a 3D CFD software. It is based on finite volume time marching method and includes several loss models such as shroud and tip leakage flow, MULTALL has been created and enhanced continously by Professor Emeritus John D. Denton since the 1970's. Minor changes was done to MULTALL such as regulating the convergence.

3.4. STAR-CCM+

STAR-CCM+ is a commercial computer aided engineering software owned and distributed by SIEMENS and is used in many engineering applications within flow mechanics. The final validation is performed in this software and the flow case described in the theory is covered in STAR-CCM+ through energy equations, flow models etc. STAR-CCM+ can employ multiple different turbulence models but the one used was k-ϵ turbulence model.

3.5. Work Flow

With the sufficient theory being researched and the application is settled for the designer, it is still not a straight forward task of designing a turbine. The software used are divided in a logical way which makes it easier to divide the course of action into multiple routines. The designing approach is best illustrated through the schematics below, starting from the top at I.

The operating points in which the turbine is supposed to work in is set by the engine and the turbocharger, meaning that they are governing the pressure, temperature and other data. Coming from stage I the values set are used in MEANGEN (II) and a preliminary design was constructed. MEANGEN gives preliminary output values such as exit mach number, stage reaction, stage loading, flow coefficient and many more. The blade design was then generated in STAGEN (III) and a first glance of the design is given. If the design is not favorable some design parameters in MEANGEN and STAGEN can be edited such as maximum thickness, leading edge shape or the flow angles. MULTALL provides a quick 3D CFD simulation that takes about 5-20 minutes in a typical Linux machine in 2020 depending on the flow case. With a fast converging software the performance can early on be scrutinized. The effects of changing blade design is therefore also simple. In the case of finding the preferable working condition stage I-III was iterated until optimum was found. When a particular design was chosen the blade geometry was then extracted to STAR-CCM+ and a final simulation was performed. A mesh independence analysis was made in STAR-CCM+ first. This is typically made by creating models with

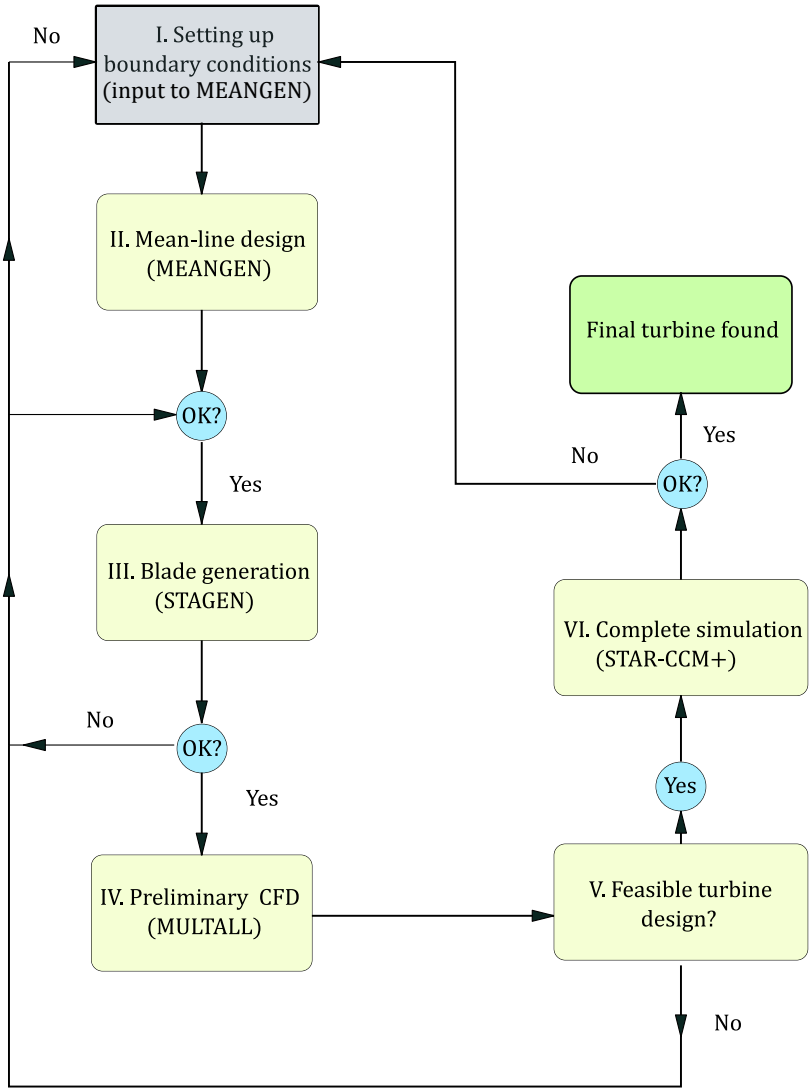

Figure 3.1.: Work flow used in this thesis starting from I to VI

different amount of mesh elements, thus reducing the mesh size where a finer mesh gives more accurate results. The result from STAR-CCM+ was compared to the result from MULTALL. If the result looked reasonable both by comparing state V to VI together with convergence plots, the result could be further investigated. MULTALL is provided with plotting functions that are difficult to create in STAR-CCM+ and MULTALL was therefore used to analyse the result such as flow angles, contour plots, loading diagrams etc.

3.6. Operating Conditions

There were five particular cases given from Volvo in which the truck is supposed to operate within, containing cases with high loads at low engine speed and low load at high engine speed and cases in between. In the engine the flow is always pulsating but these flow cases are averaged to represent steady state scenarios.

Table 3.1.: Cases to be studied

Cases	PR	T_{in} [K]	$\dot{m}$ [kg/s]	N [rpm]
A	1.497	472	0.27	21600
B	1.339	653	0.25	28800
C	1.094	549	0.13	28800
D	1.658	778	0.38	28800
E	1.677	720	0.39	40800

The data from these five cases will be used for operating points in which the turbine is designed to operate. The objective is to create a turbine that operates well for all of the cases A-E and with a E-TC the rotational speed, N is treated as a free parameter. As a first glance at the problem all cases A-E was investigated with rotational speed set to vary, see section 4.3. One design case was thereafter chosen and tested with the conditions of the other cases. So a turbine based on for example case D was tested in case A, B, C and E. The turbines were designed in Denton's program package and computed through both MULTALL and STAR-CCM+.

3.6.1. Turbine Study

One of the goals was also to examine whether the design program could create a a turbine with similar characteristics as a existing TC turbine. The design report was used to fully replicate the existing turbine both in terms of inlet and outlet conditions, and also turbine design parameters such as axial chord, pitch-chord ratio etc. to ensure a similar solidity and turning. MEANGEN and STAGEN comes with many pre-chosen values and relations from John D. Denton. Some of these values and relations was not applicable to the case to be studied and the source code was edited to resemble the actual case. The final result was validated in STAR-CCM+.

3.6.2. Electric Turbo Compound

To investigate for the possibilities of an E-TC a turbine design in similarity to the existing design was used in MULTALL and the rotational speed was set as free parameter. The

different rotational speeds was simulated with different pressure ratio to capture the different operating conditions. The inlet pressure was set as constant and the outlet pressure was varied. This was carried out for the inlet temperature in case B and D. This was carried out in MULTALL.

Chapter 4.

Results & Discussion

The result is disposed by firstly covering results from the turbine study followed by the operating conditions. As the operating conditions is covered it acts as a foundation to the E-TC and two new possible E-TC is suggested. The Results is discussed together with suggestions of further improvements and the sources of error.

4.1. Case Study

The design that was chosen to resemble is shown in figure 4.1.

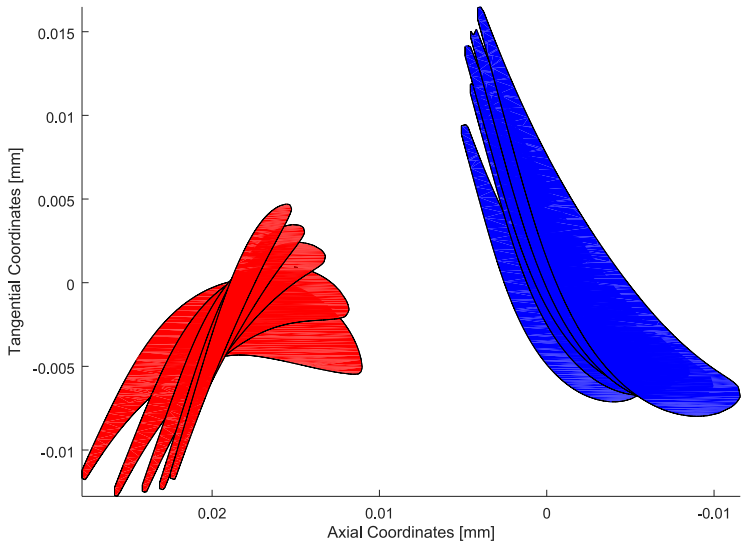

Figure 4.1.: Template design

With the correct pitch to axial chord, axial chord etc. result from MEANGEN and STAGEN is shown below:

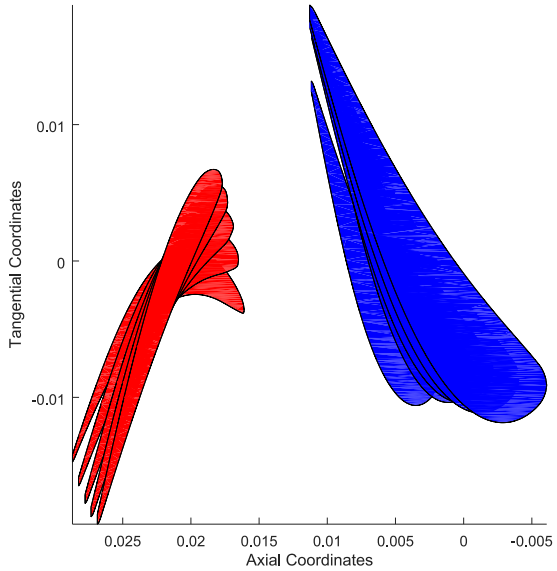

Figure 4.2.: New design from MEANGEN and STAGEN

These turbines was computed in MULTALL and the results were following:

The new turbine shows a minute difference in efficiency. The coordinates for the models was then exported to STAR-CCM+ for a full analysis. Unfortunately, new design model caused an error in STAR-CCM+ as the swallowing capacity was not sufficient. As described earlier, some modifications was made in the source code of MEANGEN. One of the fundamental alterations are the reduction of hade angles, meaning the outer and inner wall angles, see figure 4.3. Typically in turbine design the turbine channel is constructed as a diverging section. This is a feature to better account for secondary losses and tip clearance losses as the gas expands through the turbine. This would argue that the changes made in MEANGEN constructed a turbine with a smaller swallowing capacity than the design otherwise would have made and therefore this was not shown in MULTALL.

As the hade angle, ϵ, is reduced to zero, the diverging section is removed and the turbine is purely cylindrical. Altough MEANGEN and STAGEN could construct a turbine without hade angles, the effects of this could not be accounted for in MULTALL for this turbine design. The other major modification of the source code for this case study was the pitch to axial chord. The deficient swallowing capacity occured when the pitch to axial chord was set the same as the base design. Other turbines has been designed without hade angles but with pitch to axial chords calculated using the Zweifel criterion and the swallowing capacity was as intended. The pitch to axial chord was modified to resemble the base design to give a better comparison of how MEANGEN designs the turbine. As the standard values of the parameters used in MEANGEN are arbitrary in some sense,

Table 4.1.: Comparison between new and template design. Computed in MULTALL

Turbine	η_{ts} [%]
Template	78.71
New	78.86

the blade pitch to axial chord (and implicit the aspect ratio) was specified to resemble the base design. The result would be that the parameters left freely for MEANGEN to utilize and the design philosophy used in MEANGEN could be better than the base design. The template was designed with a software that used a different variation in pitch to axial chord. The meridional view of the designs show the differences. MEANGEN uses a meanline calculated pitch to axial chord ratio together with quasi-orthogonal angles to describe the pitch to axial chord ratios.

This results is a longer true chord in every section which figure 4.1 and 4.2 and tighter throat in the rotor. The use of quasi-orthogonal angles and the pitch to axial chord limits the ways to avoid this but it should be possible to have high a high swallowing capacity with this pitch to axial chord distribution. There should not be any problem to change this in the source code to MEANGEN but to the extent of this thesis and the time frame it would not be reasonable to change this. Instead, one could use the equations already given in MEANGEN that relates the solidity and Zweifel cofficients.
When instead using the predefined values from the source code in MEANGEN and STAGEN, a turbine, which had a differing pitch to chord and solidity gave an total to static efficiency of 78% in MULTALL.
The results from MULTALL and STAR-CCM+ differs with almost 1 percentage point. Table 4.2 shows the torque and temperature based efficiencies obtained in STAR-CCM+ to give a sense of how the result differ from MULTALL and STAR-CCM+.

Note that the torque-based total to static efficiency is the most suitable for comparison to MULTALL's temperature-based total to static efficiency in table 4.1. This shows the validity of MULTALL as an valid early CFD-tool in the design process.

4.2. Operating Conditions

The differrent flow cases described in table 3.1 can be favorable to describe in terms of stage loading and flow coefficient and use the Smith chart.

Comparing case A and C in stage loading, with A having a very large stage loading. This comes from the low revolution speed of 21 600 rpm which have a large effect on the stage loading as the blade speed is squared in the definition, see (2.31). The flow coefficient for case A is larger than case D which also comes from the lower revolution speed. Meanwhile, the mass flow for case C is smaller which gives C a lower flow coefficient. The low stage loading comes from the low stage enthalpy drop, hence the

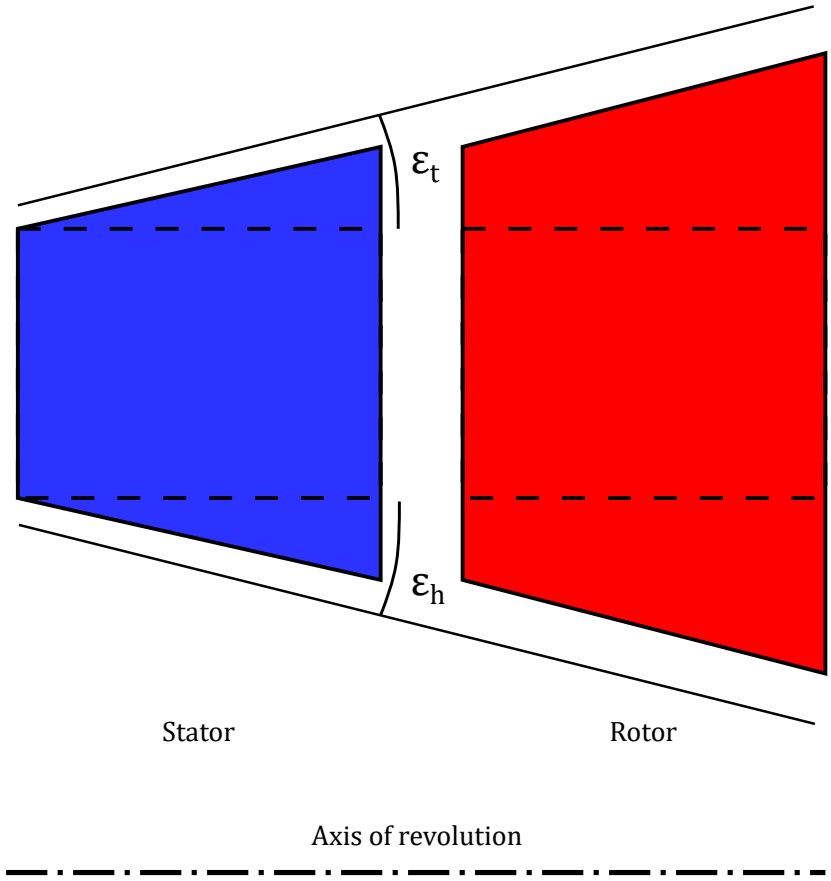

Figure 4.3.: Meridional view of turbine channel with hade tip and hub hade angles compared to cylindrical turbine (dashed line)

low pressure ratio. Case D has a large stage loading which comes from the large enthalpy drop compared and lower revolution speed of 28800 rpm than for example case E that has both a high stage enthalpy drop and a high revolution speed 40600 rpm. If reasoning with the theory of the Smith chart in mind, the properties of case A and D should provide a less efficient turbine as more secondary losses will occur, whereas case C should have a larger efficient. One could create a design for turbine case C but as this is a case which is less important for the overall driving cycle and it is not certain that this design would be suitable for the other cases.

One should not compare these data to the original Smith chart, figure 2.7, and hope for a similar outcome in efficiency as the original Smith chart contains turbines that have other

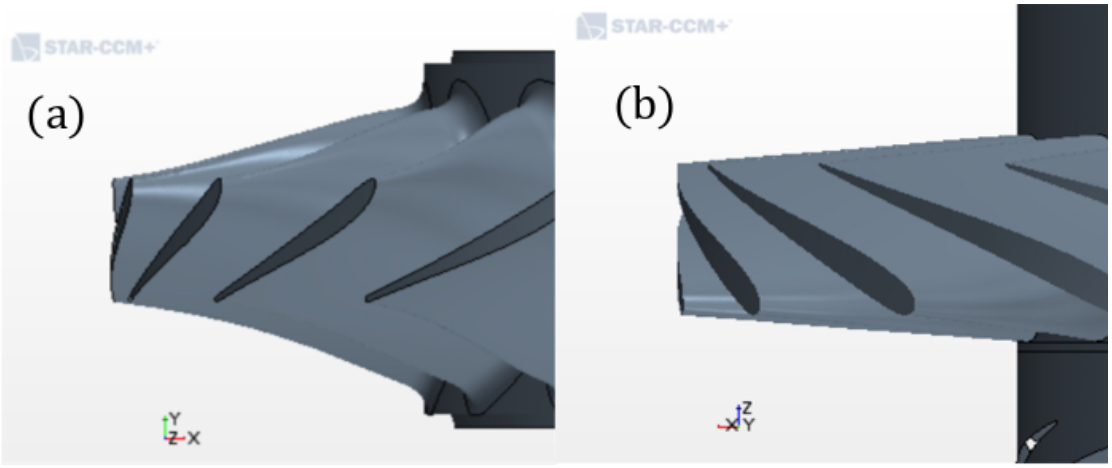

Figure 4.4.: Quasi-orthogonal view of the rotor blade: (a) template, (b) new design

attributes such as zero tip clearance, constant axial velocity and others. From the 5 cases, case D is considered to be the most important to ensure high efficiency in. Therefore, the inlet conditions from case D for $N = 57600$ was used to create a turbine and test it through the other cases. The efficiency is calculated through STAR-CCM+ and is shown in figure 4.6 below and the design was made with tip clearance of 0.45 mm.

One can note that some cases are very difficult to maintain a high efficiency such as case A and C. Flow case A is characterized revolution speed and flow case C is characterized by low pressure and mass flow. As an effect of choosing a higher design rotational speed for case D, the turbine efficiency is similar to case E. By increasing the revolution speed the stage loading for case D turns into $\psi = 0.88$ and $\phi = 0.31$.

4.3. Electric Turbo Compound

The different cases that was studied earlier was used to investigate the influence of rotational speed N to the efficiency. The flow cases should all have their individual optimum design and as N is important in the design, each case and N set as a free parameter recieved their specific design from MEANGEN and STAGEN. The result below was calcultaed in MULTALL.

The designs for these simulations had zero tip clearance and the efficiencies should be regarded only in relationship to the rotational speed. An increase in rotational speed gives a higher efficiency with a drastic drop after 60 000 rpm. One should note that the change in efficiency is less than 1 percentage point in the span of 30 000 to 60 000 rpm.

As in previous section, case D was chosen to be most important to account for and a design was chosen for case D with 57 600 rpm as the design rotational speed N_{des}. The chosen rotational speed was based on a design report and with figure 4.7 showing that

Table 4.2.: Result for the template design. Calculated in STAR-CCM+

Turbine	η_{ts} [%]	$\eta_{ts,tq}$ [%]
Template	78.7	77.6

maximum efficiency is obtained in the vicinity. Figure 4.8 below shows the result from using a turbine design based on case D and running the turbine with inlet conditions for the other flow cases. The rotational speed was varied as the inlet conditions was kept constant. Figure 4.8 is based on a turbine with zero tip clearance.

Figure 4.8 shows optima at 50 000 rpm and 55 000 rpm. Case C needs a far lower rotational speed at 20 000 rpm. This is very reasonable since this case operates with low loadings and therefore will need a lower rpm.

4.3.1. E-TC Design Study

Now that the influence of rotational speed and flow case has been established, it is about time to implement the findings into new possible E-TC units. Two new designs has been designed by using figure 4.7. Case D is still of interest but now two different designs are made. One designed for a $N_{des} = 35000rpm$ (called TL as in Turbine low revolution speed) and one designed for $N_{des} = 55000rpm$ (called TH similarily). TL and TH designs was also made differently in the chosen flow angles. The flow angles was chosen through a parameter study and its influence of the efficiency. Now that the aim is to provide two reasonable turbines, the tip clearance is added with a clearance of 0.45 mm.

Instead of considering different cases one can look at the pressure ratio as a free parameter and vary the corrected speed meaning that 50% is the corrected speed $N/\sqrt{T_{01}}$ is 50% of the design case. The figure below shows the result for TH

Figure 4.9 shows that for a particular pressure ratio the turbine can switch the rotational speed. This representation could be deemed of same character as figure 4.8 but now the result can be more quantified for the programming of the E-TC. As the pressure ratio varies, the E-TC can use results from plots as figure 4.9 to adjust the rotational speed and maximize the efficiency.

This behaviour comes from the flow angles as the change in pressure ratio and temperature difference varies, the stage loading, reaction and flow coefficient will vary. Considering the relationship between stage loading, rotational speed and the enthalpy change in equation (2.31). Looking at the flow case for 50% speed, at pressure ratio 1.35. As the rotational can freely vary, the turbine must increase its rotational speed to 90% of N_{des}. Figure 4.11 shows the pitchwise flow relative flow angles. Figure 4.11 was obtained through MULTALL.

Where I, J, K are the variables for the cylindrical coordinates used in MULTALL with

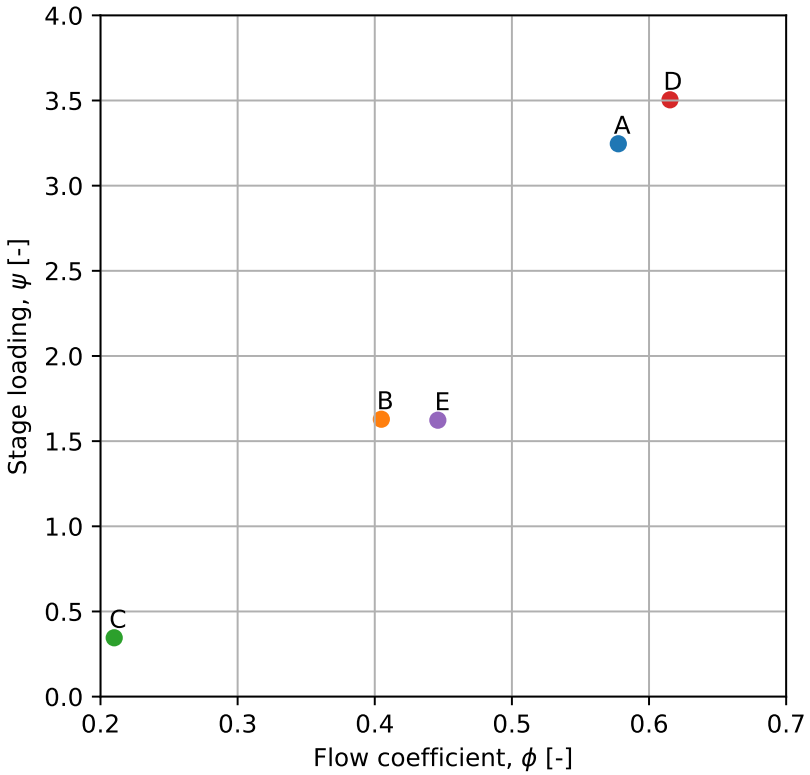

Figure 4.5.: Smith chart for the flow cases

"J" representing the the axial position, "I" pitch-wise position and "K" will be referred to as the span-wise position. The parameter I goes from 1 to 37 with 1 being the suction side of the blade and 37 is the pressure side. J is described in table below:

The result in figure 4.11 below is calculated through MULTALL. TH was designed for a inlet rotor angle of approximately 71°

Similar plot but with a 90% corrected speed is shown below, also calculated in MULTALL. Figures such as 4.11 and 4.16 is obtained through a plot function in Denton's software package that uses the result calculated in MULTALL.

A comparison between figure 4.11 and 4.12 shows that the flow angles are more "aligned" with the design point when the rotational speed is increased at 1.35 bar. Even though some deviation exists at the hub it is still a great improvement in the efficiency. Turbine TL behaves similarily as shown below and this turbine was designed for an inlet rotor angle of 69°:

TL was also examined through a second flow case, more precisely being flow case B inlet conditions:

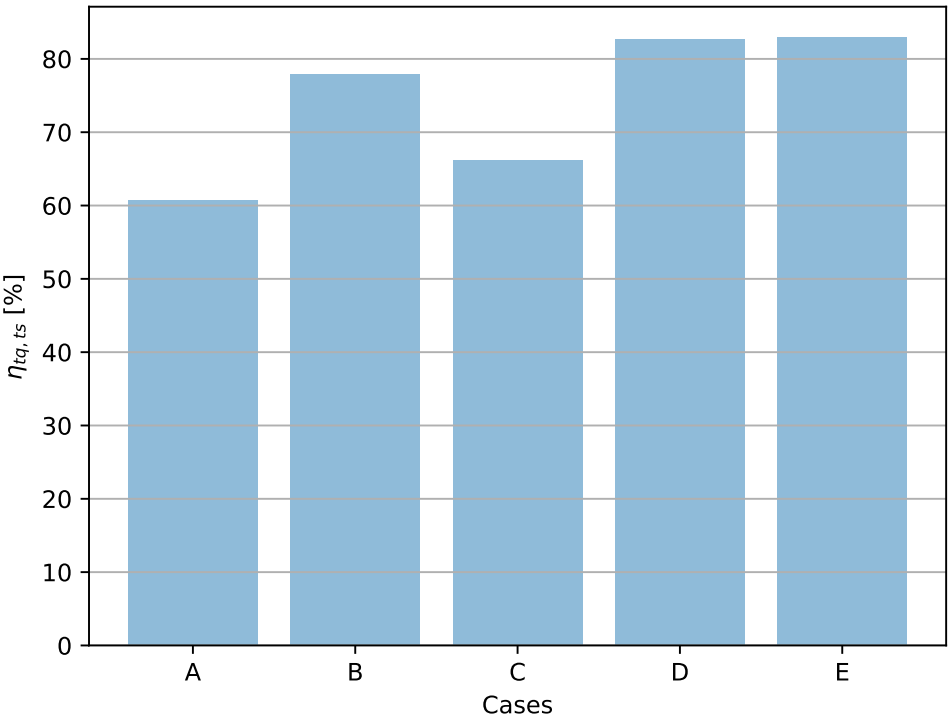

Figure 4.6.: Efficiency of a turbine based on flow case D and runned through all flow cases. Calculated in STAR-CCM+.

The behaviour is similar to figure 4.9. The local maximum at 50% would also occur if lower PR was calculated but since the turbine normally not operates under such circumstances. A step of 0.1 in pressure ratio was deemed sufficient for illustrating the behaviour. As the plots show, the efficiency increases with pressure ratio and corrected speed and an optimum occurs for each flow case. Saravanmutto et. al. [9] states, as the flow accelerates, the turbine can operate over a wider range of incidence without any large increases in losses.

Figure 4.15 shows the spanwise incidence for the design case where the inlet rotor angle was chosen as 69°.

The spanwise entropy loss coefficient for the design case is shown in figure 4.16.

Corresponding incidence plot is shown in figure 4.17 below:

One can note a increase in incidence as the turbine operates off design when comparing figure 4.17 and 4.15. Figure 4.18 shows the spanwise entropy losses for the flow case 98% at $PR = 1.5$ from figure 4.14

Figure 4.19 below shows similar plot for flow case $N/\sqrt{T_{01}} = 164\%$ of the design case:

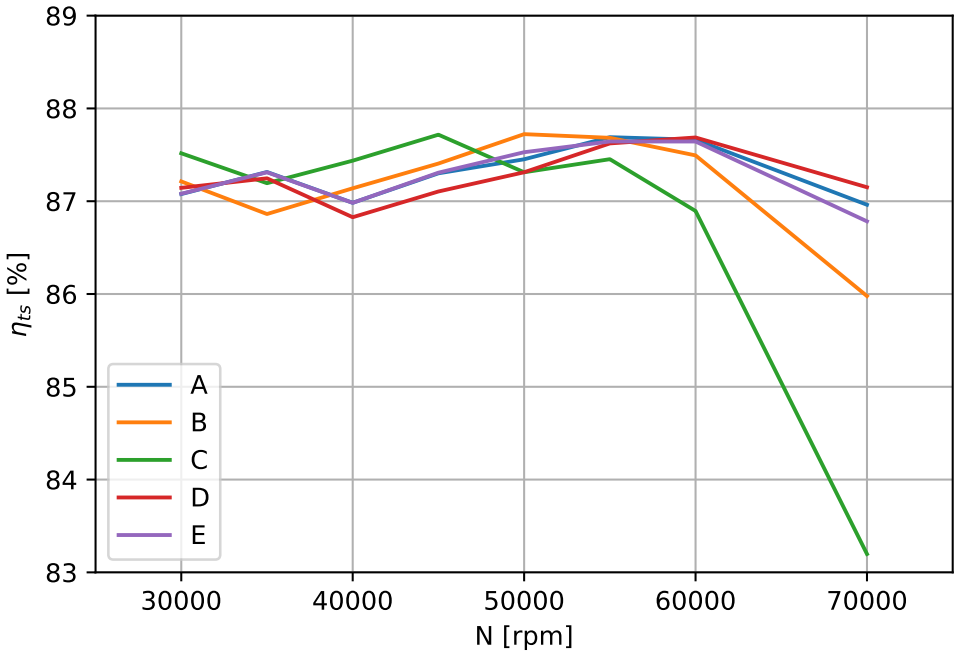

Figure 4.7.: Different turbine designs for each flow case A-E and rotational speed, 40 in total. Calculated in MULTALL.

The spanwise entropy generation for the flow case $N^* = 164\%$ is shown below:

One can see an increase in the peak entropy when increasing the corrected speed but also an increase in incidence when having a lower corrected speed. These result is necessary in designing the E-TC as for each new temperature inlet, N^* will change as the true rotational speed must vary along with T_{01} and the end goal is to minimize the incidence.

The off-design stage loading in the flow case D for TH turbine is shown in figure below and is calculated through the result from MULTALL.

Figure 4.22 shows the similar plot for TL and flow case A.

Similar plot is obtained for TH and flow case B:

Figure 4.22 and 4.23 shows that optimum off design is occurs in at a stage loading at about 1 and up to 1.2 whereas figure 4.21 suggests a maximum efficiency at approximately 0.8-0.9. Table 4.4 shows the design stage loading at mid span from the definition, equation (2.31).

This could argue for that TL has a too low stage loading due to the low rotational speed chosen. For TH the optimal stage loading is reached when the flow case approaches the designed stage loading.

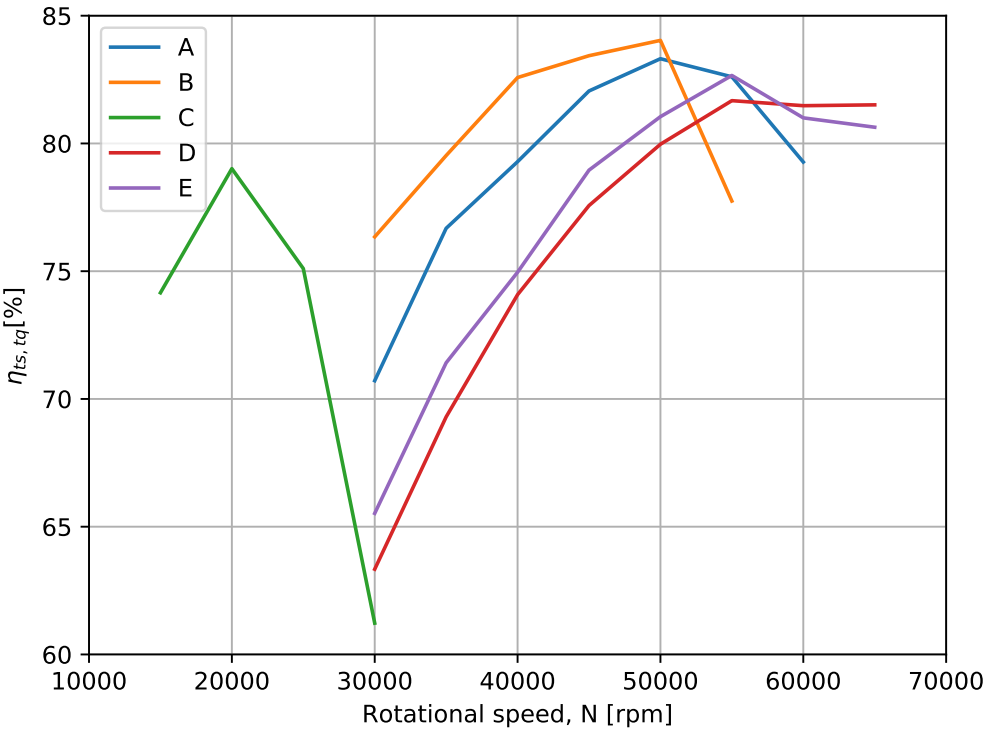

Figure 4.8.: Parameter study of rotational speed on the different cases. Calculated in STAR-CCM+.

One important trend that should be noted is that a design with a low will have to operate with an overall revolution speed above the designed speed. Figure 4.9 shows that a turbine with a high N_{des} is better adapted to flow cases that needs the turbine to decrease N. For example, TL peak efficiency at 90% corrected speed is approximately 77.2% at a pressure ratio of 1.18 and TH peak efficiency at 90% is 78.5% with a pressure ratio of 1.35. The transition to overspeed must occur (in terms of PR) earlier for TL than TH.

Looking into the corrected mass flow, i.e swallowing capacity of the new turbines, figure 4.24 shows the corrected mass flow for each corrected speed. The result below is obtained from MULTALL. Pressure is set to bar, to reduce the decimals for corrected mass flow.

Similar plot for TL and case D.

The same type of plot can be made with TL for inlet case B but since the result is displayed in corrected terms the behaviour will not behave significantly different. These plots can show that the turbines corrected mass flow are starting to stagnate at pressure ratios larger than 1.7 or 1.8 meaning that the turbine chokes. The choking can occur in the nozzle throat or at the turbine outlet. If the turbine chokes at the nozzle, the corrected mass flow for each corrected speed will converge to one horizontal line [9]. The plots

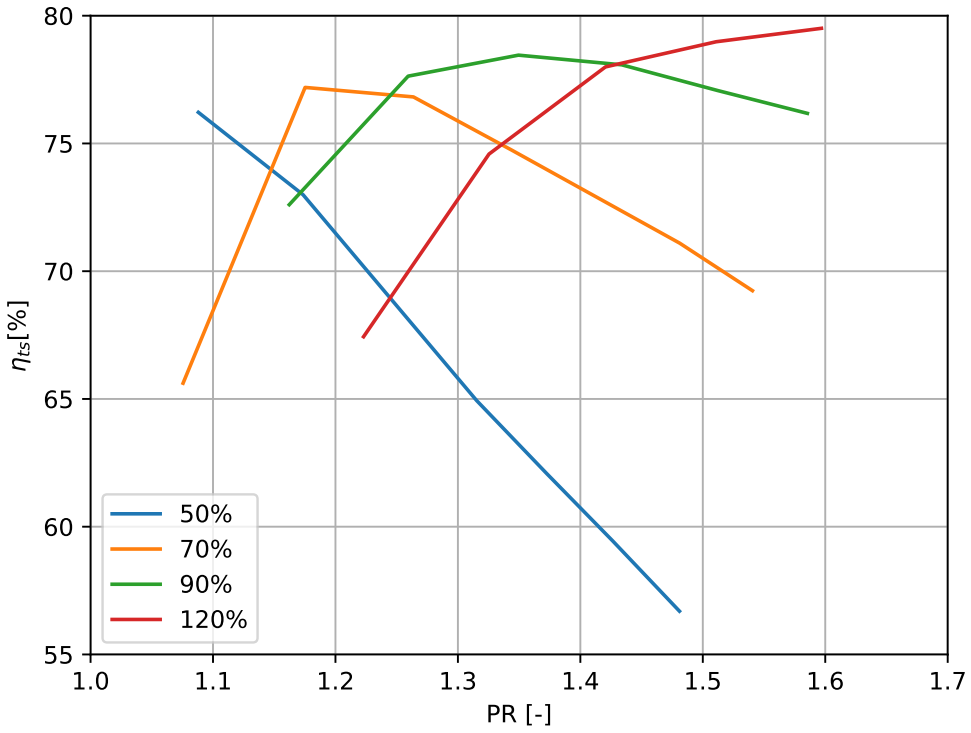

Figure 4.9.: Efficiency as a function of the pressure ratio for different corrected speeds, TH Calculated in MULTALL.

could be expanded to larger pressure ratios but since the turbine seldom operates in pressure ratios larger than 1.7 it was not considered. Figure 4.25 shows an unexpected behaviour with the low corrected speed 50% having a larger swallowing capacity than the plots for larger corrected speed. The swallowing capacity should decrease with corrected speed and at a certain pressure ratio the corrected mass flow should stagnate. Figure 4.24 indicates that choking occurs in the nozzle throat but the figure does not either follow the result as expected with the corrected speed at 50% of the design case has a larger swallowing capacity than 70% and 90% of the design corrected speed. Another turbine designed in MEANGEN and STAGEN but computed in both MULTALL and STAR-CCM is shown in figure 4.26.

The characteristics of the turbine in terms of design and size shall not be discussed but for the sake of argument this plot shows that the swallowing capacity is slightly lower when calculating in MULTALL compared to the calculations from STAR-CCM+. The result calculated in STAR-CCM+ behaves more as expected with the corrected mass flow converging to one line. The difference in swallowing capacity computed by MULTALL and STAR-CCM+ could be an effect of the implementation of gas properties. The calculations in MULTALL was made with a $C_p = 1133 J/kgK$ and

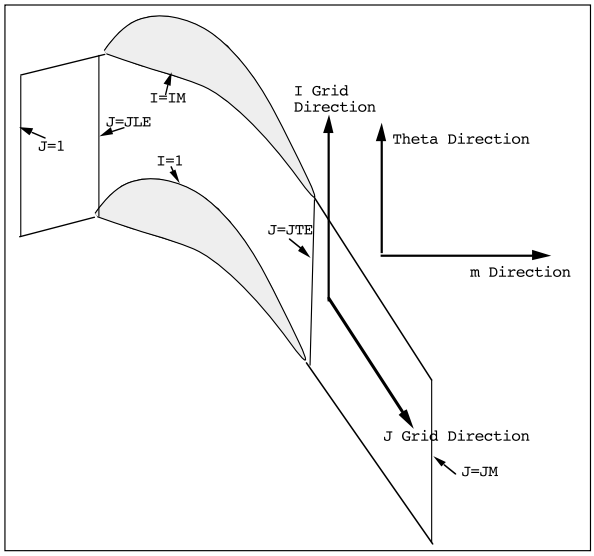

(a) Blade to blade view

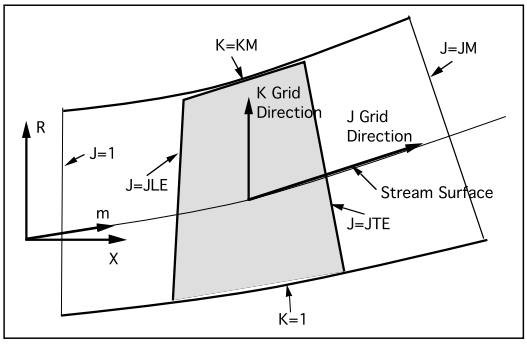

(b) Meridional view

Figure 4.10.: MULTALL nomenclature [20]

$\gamma = 1.34$. STAR-CCM+ computed these values to aproximately $C_p = 1100 J/kgK$ and $\gamma = 1.35$. The specific heat and heat capacity ratio obtained by STAR-CCM+ was used in MULTALL with a minute effect of the swallowing capacity.

4.4. Further Improvements

The comparison between the new design and the template could be further improved by looking more into blade parameters such as thickness distributions, maximum thickness and its position. One apparent thing when looking at the blade sections at figure 4.2 the

Table 4.3.: Description of index J and its position throughout the turbine stage

Inlet	LE Stator	TE Stator	LE Rotor	TE Rotor	Outlet
1	26	96	132	202	222

rotor leading edge is very sharp for the sections near the hub. This is a good aspect when designing a turbine that does not to be robust against incidences. But the design shown is probably too sharp in a manufacturing point of view and the leading edge thickness should therefore be reconsidered in a possible new design.

The E-TC designs suggested in this thesis will increase the overall efficiency by monitoring the revolution speed of the turbine. It should be stressed that the E-TC turbines have not been designed for improving the peak efficiency. A turbine design for broad ranges of operating points is typically characterized by a blunt leading edge which it more insensitive to incidences that comes from off-design operation. The designs should therefore be further investigated to edit the blade design parameters such as blade thickness, leading edge thickness etc. MEANGEN is a meanline design tool which utilizes the design paramaters from one chosen section to all other sections. This makes it difficult to let certain design parameters vary spanwise and also the maximum thickness position. The strength of the meanline design is that the software could be used and manipulated into creating an optimizer which screens multiple parameters and its influence on the performance.

The blade stacking feature was used in a parameter study to investigate its influence of the efficiency and an increase in efficiency of +1 percentage point could be made. This was not used in the final comparison shown in the result which shows that the new design could be further improved.

Flow case D was chosen for the turbines created in this thesis as flow case D was estimated to be most important to design for. This was a very simplistic estimation that was based on a quantitative guessing from previous studies made at Volvo. The choosing of flow case could instead be made more rigorously by taking BSFC into considerations. A turbine could instead be chosen for a flow case where the BSFC is high and also how much the work output from the TC turbine contributes to the engine power output. This was not done because it would stretch the width of this thesis to a unmanageable amount.

Another important consideration that has not been made due to the restrictions for this thesis is the mechanical stresses. One should for further work ahead examine $\sigma \propto AN^2$ and how turbine TH's and TL's structural integrity is affected by the broad ranges in N.

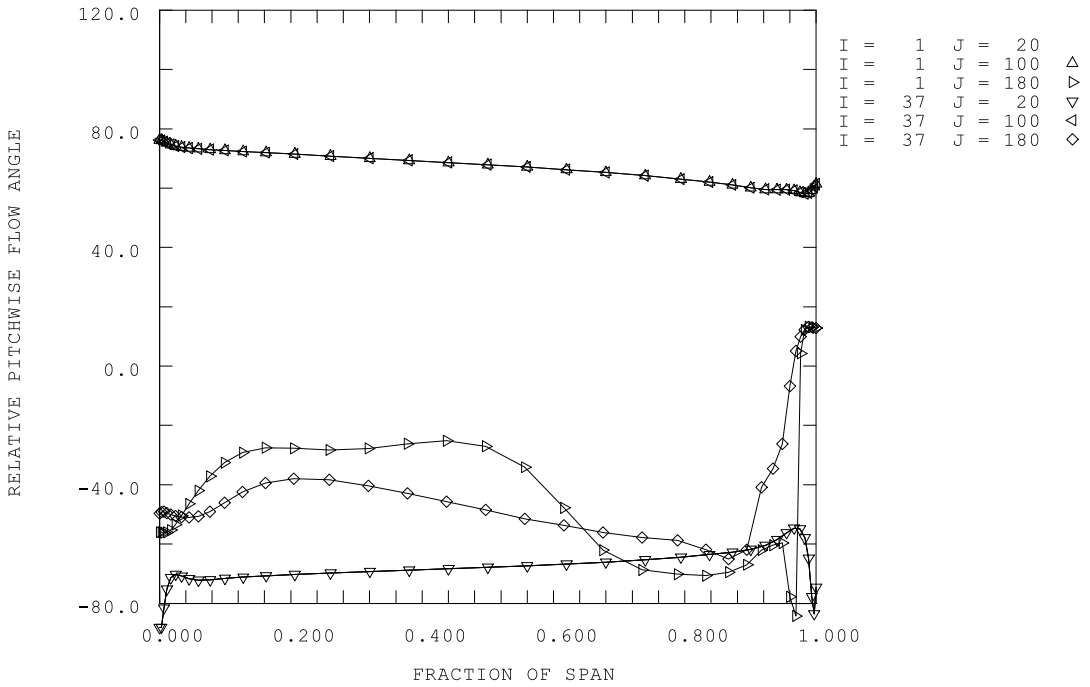

Figure 4.11.: Spanwise (0 = hub, 1 = tip) relative flow angle for TH at approximately $PR = 1.35$ and $N/\sqrt{T_{01}} = 50\%$ of the design case, TH.

The turbine created for figure 4.8 shows a peak efficiency of approximately 84% and it should be of great interest to investigate the properties of this model. Similar plots of corrected speed versus pressure ratio would be interesting to examine and this turbine may be an appropriate alternative to TH.

4.5. Sources of Error

The apparent sources of errors that affected the theory applied to the result is covered in this section.

4.5.1. Case Study

As described in the MEANGEN manual, the turbine design is performed through the assumption of constant axial velocity. Equation (2.32) shows that if the inlet angle is zero the design stage loading will always be equal to unity. The stagnation enthalpy drop is thereafter calculated through equation (2.31). One should therefore be cautious of what the meanline design calculates in comparison what is obtained after MULTALL.

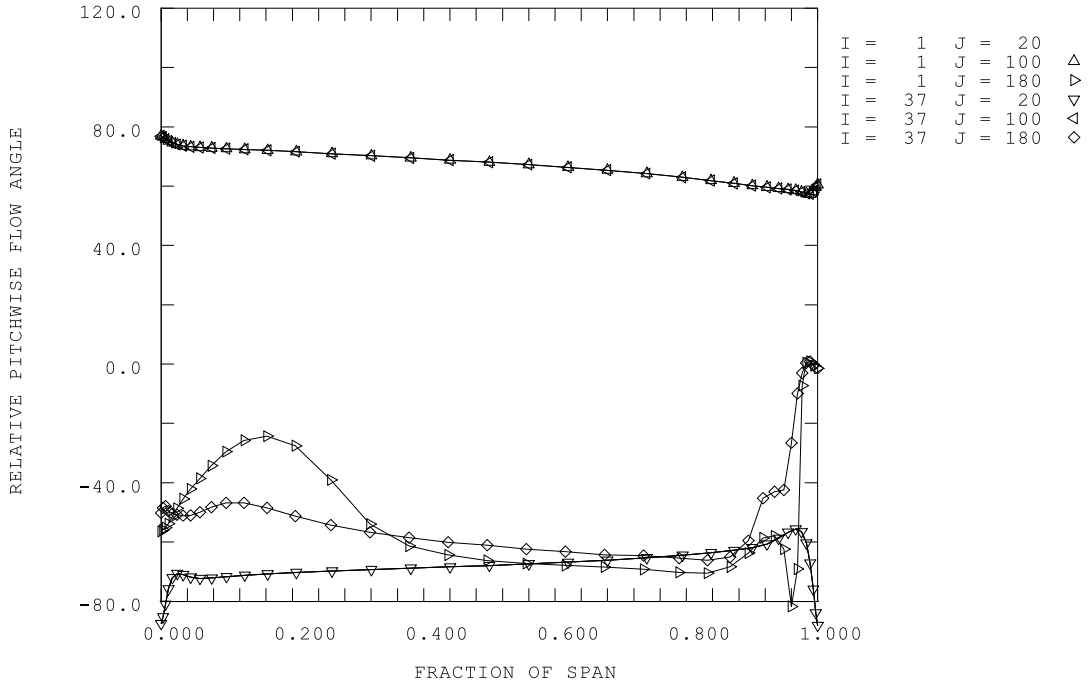

Figure 4.12.: Spanwise (0 = hub, 1 = tip) relative flow angle for TH at approximately $PR = 1.35$ and $N/\sqrt{T_{01}}$ = 90% of the design case. Calculated in MULTALL.

4.5.2. MULTALL

In the discussion about the turbine with too low swallowing capacity in the result, the effect of hade angles was ventilated. MEANGEN uses mass flow as an input parameter to calculate the hade angles. The mass flow chosen for the meanline design should however not be mistaken as the chosen mass flow for the turbine as an end result. In MULTALL a new mass flow is calculated for the turbine. This new mass flow could be affected by the removal of hade angles as the turbine has a reduced swallowing capacity. One can not exclude to possibility that the modification of MEANGEN had an impact on the turbine designs and its solution schemes. However, one should stress that MULTALL is not to blame. Some apparents has been discussed with hade angles. It was though very important to modify the code into a cylindrical turbine because of manufacturing reasons. One should have modified the code in MEANGEN and run iteratively until the correct massflow was achieved in MULTALL. The discrepancy in swallowing capacity for figure 4.25-4.26 has been discussed with some possible explanations of how the gas properties are computed in MULTALL and STAR-CCM+. The gas properties was changed in MULTALL but with no significant effect. To troubleshoot this intricacy the two turbines designed, TH and TL was also designed with hade angles. The swallowing capacity for TL was increased by 12% and for TH the swallowing capacity decreased by 16% compared the original designs. This confirms the hypothesis of the discrepancy in swallowing capacities.

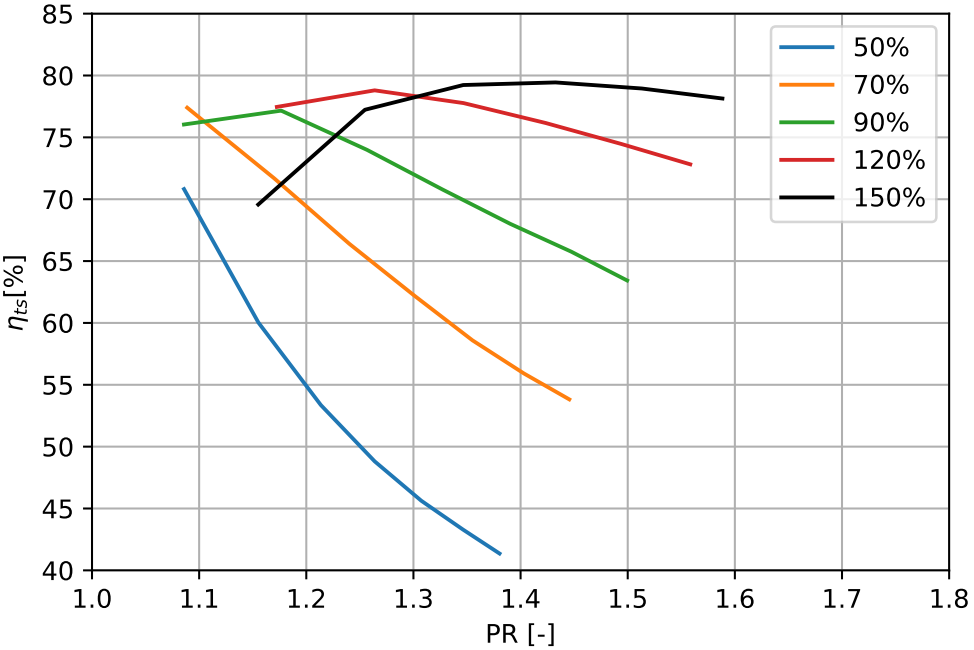

Figure 4.13.: Efficiency as function of the pressure ratio at different corrected speeds as a fraction of the design case, TL. Calculated in MULTALL.

4.5.3. Model

The model created in STAR-CCM+ consisted of a full 360° turbine with stator and rotor blades. The inlet and outlet was a simple tube neglecting the effects of inlet and exhaust duct diffusors. In this application, for most operating points, the total pressure drop in the diffuser and collector fully eliminates the static pressure recovery of these components. Therefore it can be considered sufficient to study the total-to-static efficiency of the turbine unit only. The model created in STAR-CCM+ is attached in appendices. The turbine blades that was extruded in STAR-CCM+ was also simplified as there were no chamfering used between the rotor blade and hub (and stator blade to hub and shroud). The chamfering is a feature needed for manufacturing reasons and this affects the efficiency negatively. The turbulence models used in STAR-CCM+ could be changed to Spalart-Allmaras to resemble more to what was calculated in MULTALL but since k-ϵ is typically used in the engineering department it can not be deemed as a major concern. The mesh models differs between the one used in MULTALL and STAR-CCM+ where MULTALL uses a typical H-grid for mesh and in STAR-CCM+ a polyhedral mesh was used, see appendix. STAR-CCM+ gives more options in choice of mesh and this was considered a mesh suitable for this flow case. There is also a strong possibility that the export of blade coordinates from STAGEN to STAR-CCM+ is not correctly performed. The coordinates transformation from cartesian to cylindrical coordinates is described

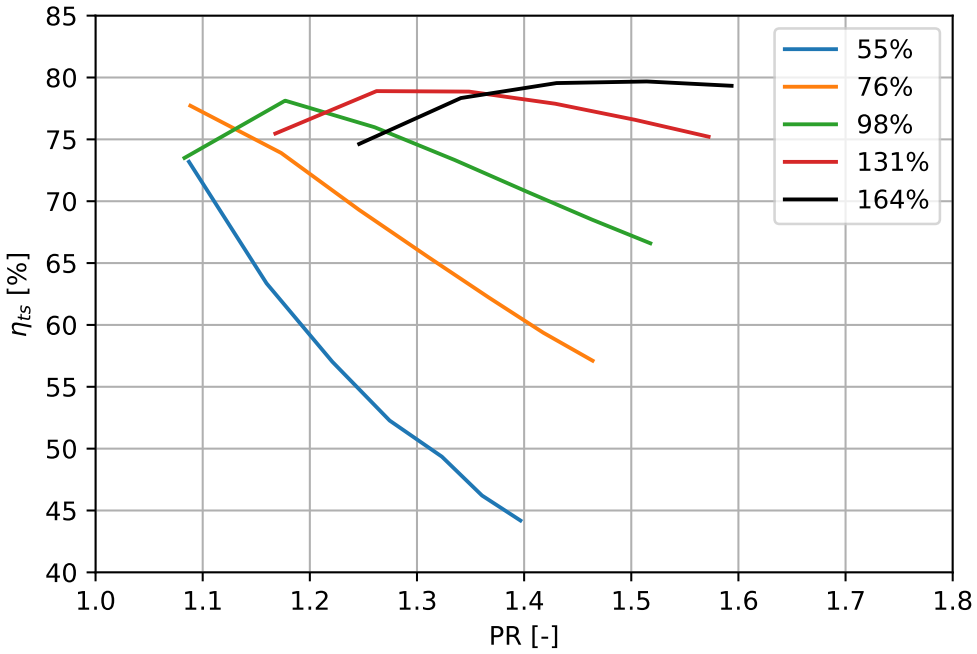

Figure 4.14.: Efficiency as function of the pressure ratio at different corrected speeds as a fraction of the design case, TL. Calculated in MULTALL.

in the description of Denton's software package and the author created a GNU Octave script that transformed the coordinates from STAGEN to a cylindrical coordinates as STAR-CCM+ require. The blades constructed through GNU Octave was compared to the plotting functions provided with STAGEN and from ocular examinations they were deemed similar.

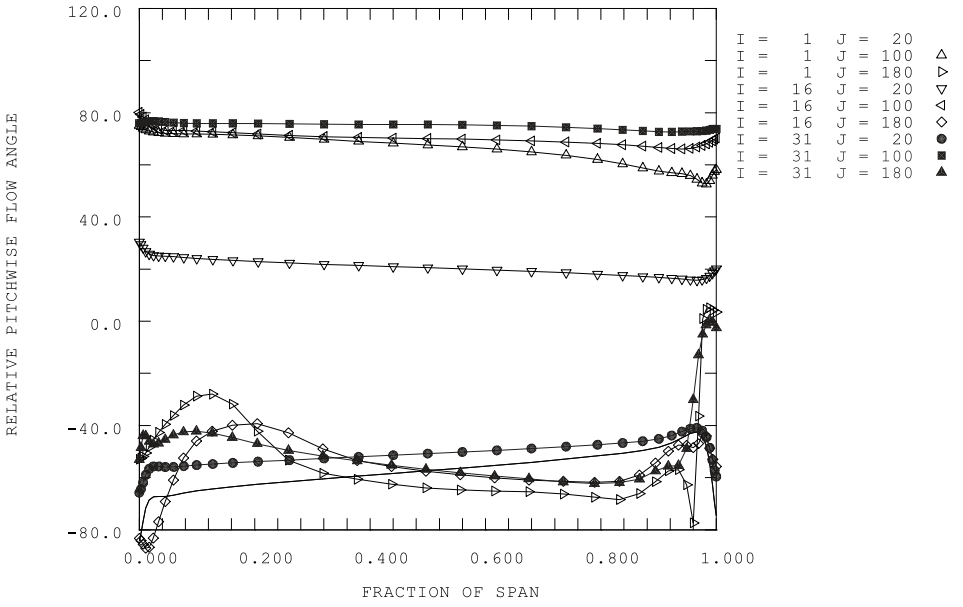

Figure 4.15.: Spanwise (0 = hub, 1 = tip) incidence for turbine at design case, TL. Calculated in MULTALL.

Table 4.4.: Design stage loading for the two E-TC designs

Turbine	ψ
TL	0.929
TH	0.918

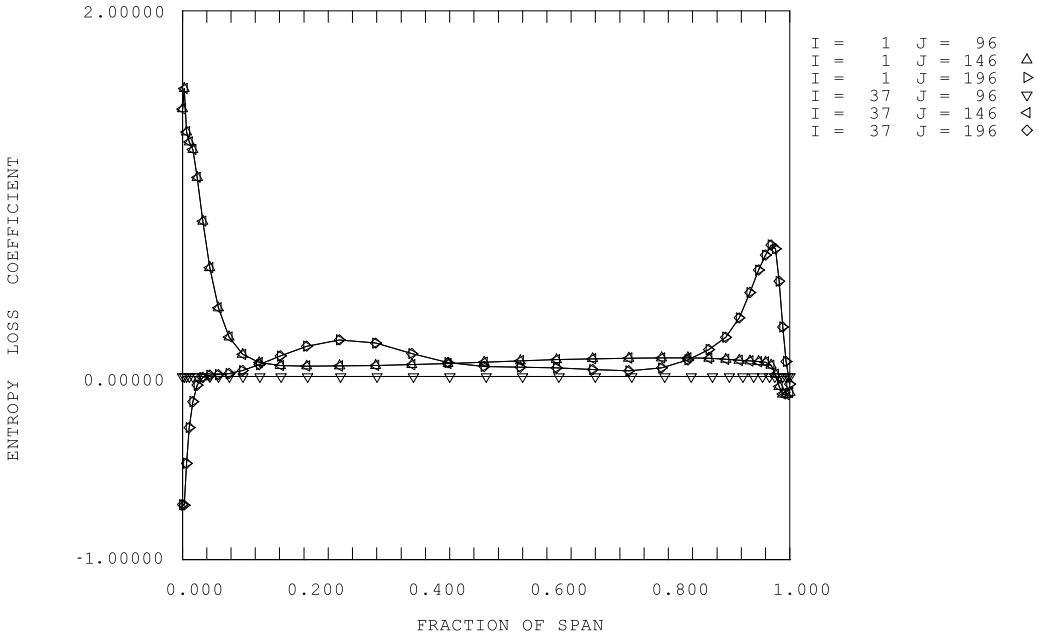

Figure 4.16.: Spanwise (0 = hub, 1 = tip) entropy loss coefficient generation at design case, TL. Calculated in MULTALL.

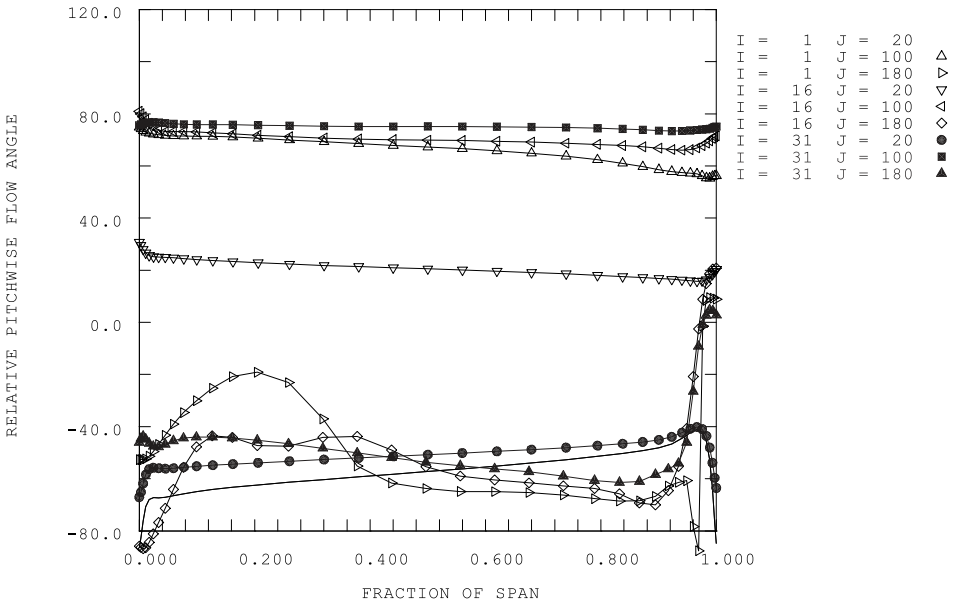

Figure 4.17.: Spanwise (0 = hub, 1 = tip) incidence plot for corrected speed $N/\sqrt{T_{01}}$ = 98% of the design case. Calculated in MULTALL.

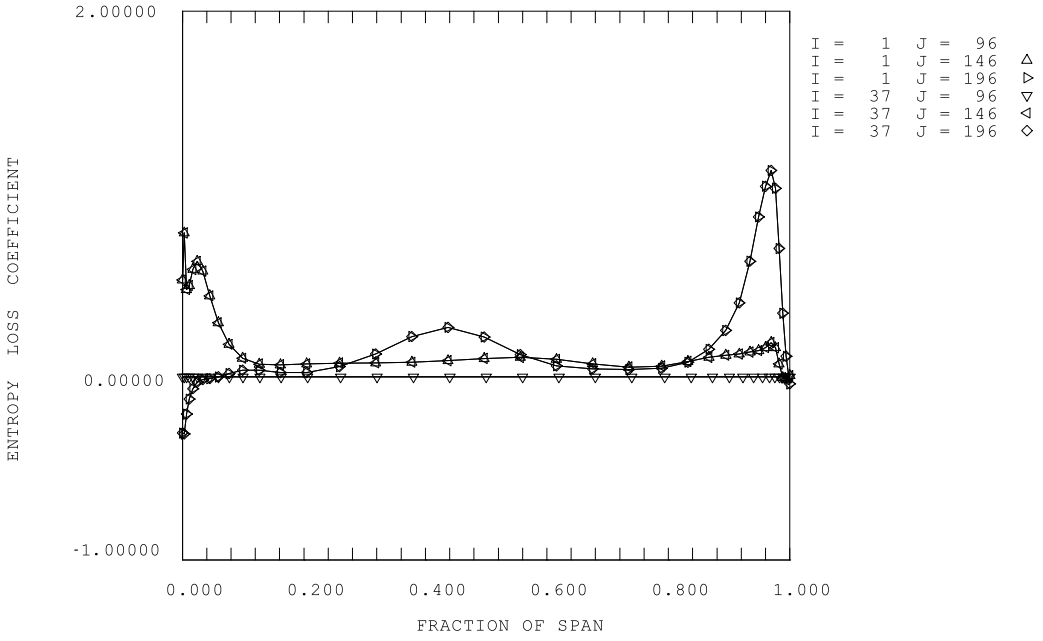

Figure 4.18.: Spanwise (0 = hub, 1 = tip) entropy increase of the rotor blade for the new design, corrected speed $N/\sqrt{T_{01}}$ = 98% of design case. Calculated in MULTALL.

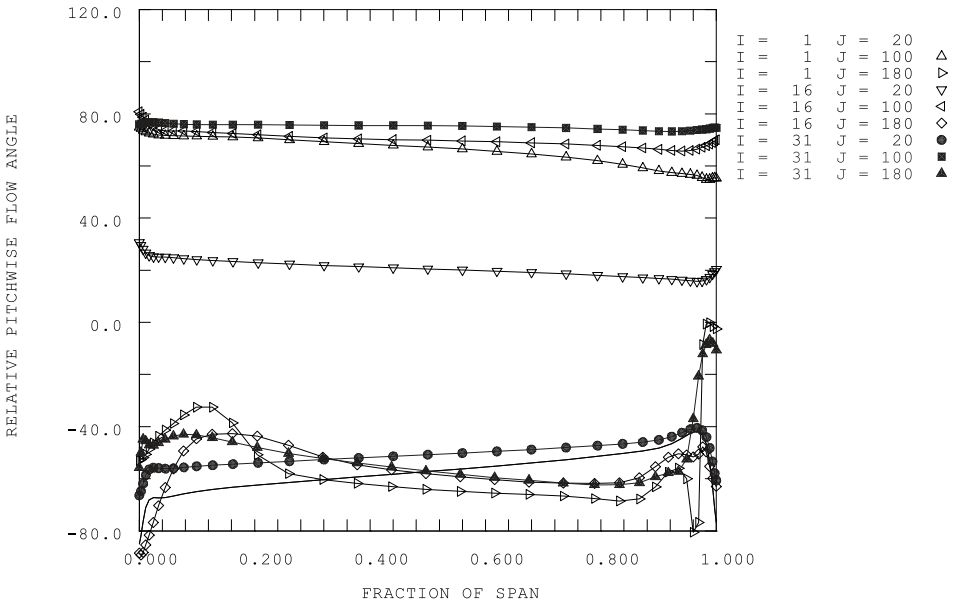

Figure 4.19.: Spanwise incidence plot for corrected speed $N/\sqrt{T_{01}}$ = 164% of the design case. Calculated in MULTALL.

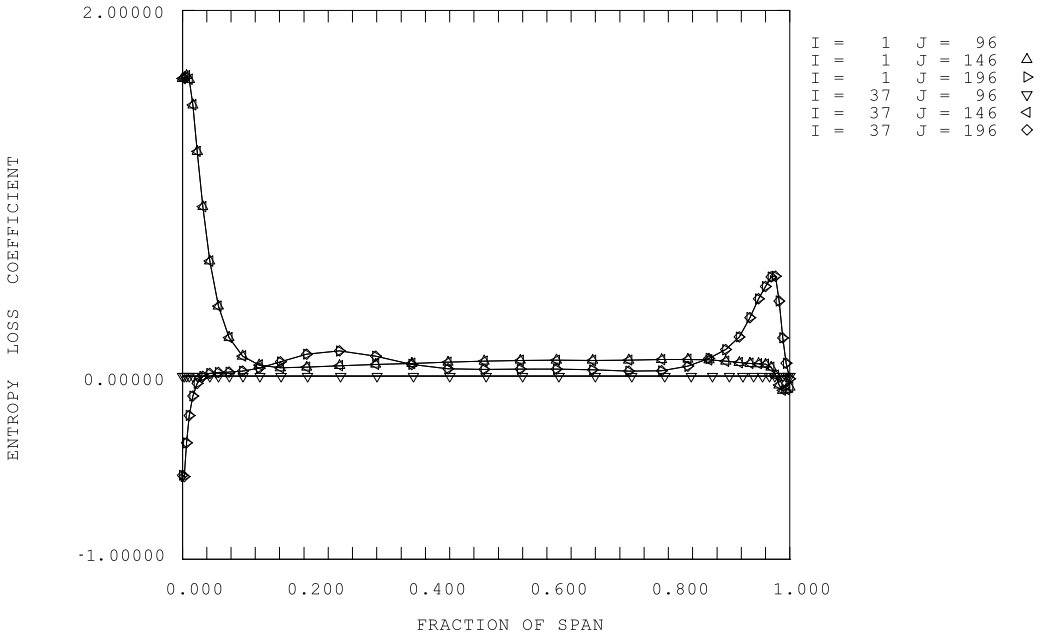

Figure 4.20.: Spanwise (0 = hub, 1 = tip) entropy increase of the rotor blade for the new design, $N/\sqrt{T_{01}}$ = 164% of the design case. Calculated in MULTALL.

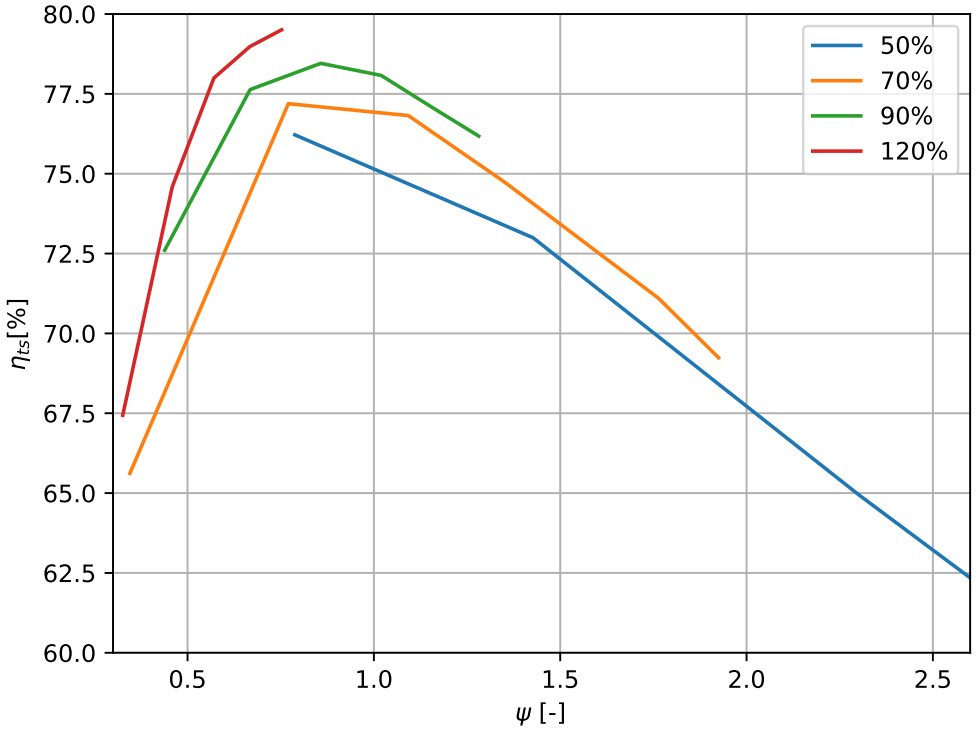

Figure 4.21.: Efficiency as a function of off design stage loading for differernt corrected speed, TH. Calculated in MULTALL.

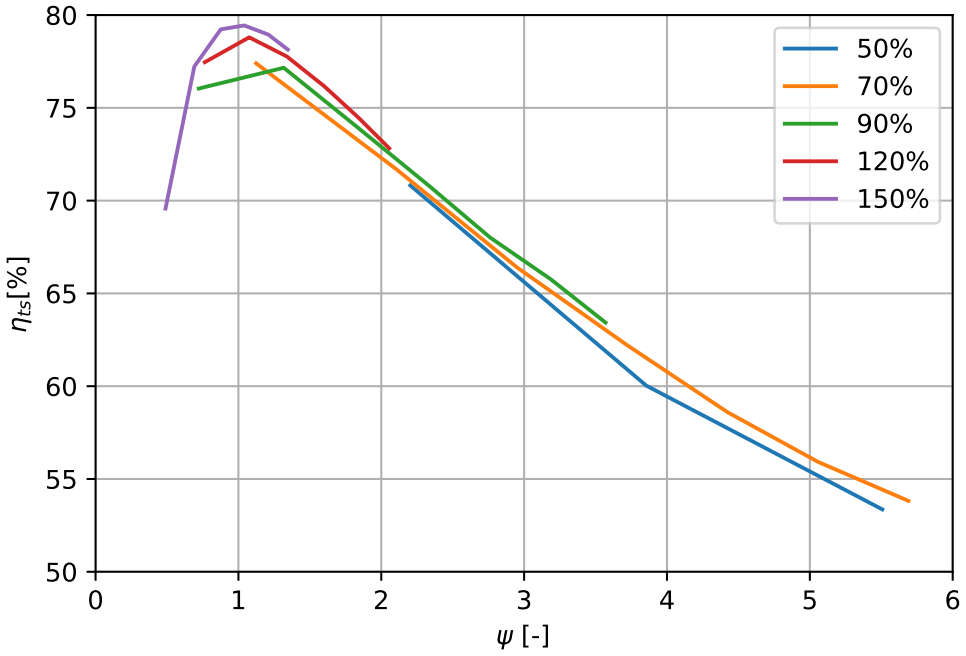

Figure 4.22.: Efficiency as a function of off design stage loading for differernt corrected speed, case D, TL. Calculated in MULTALL.

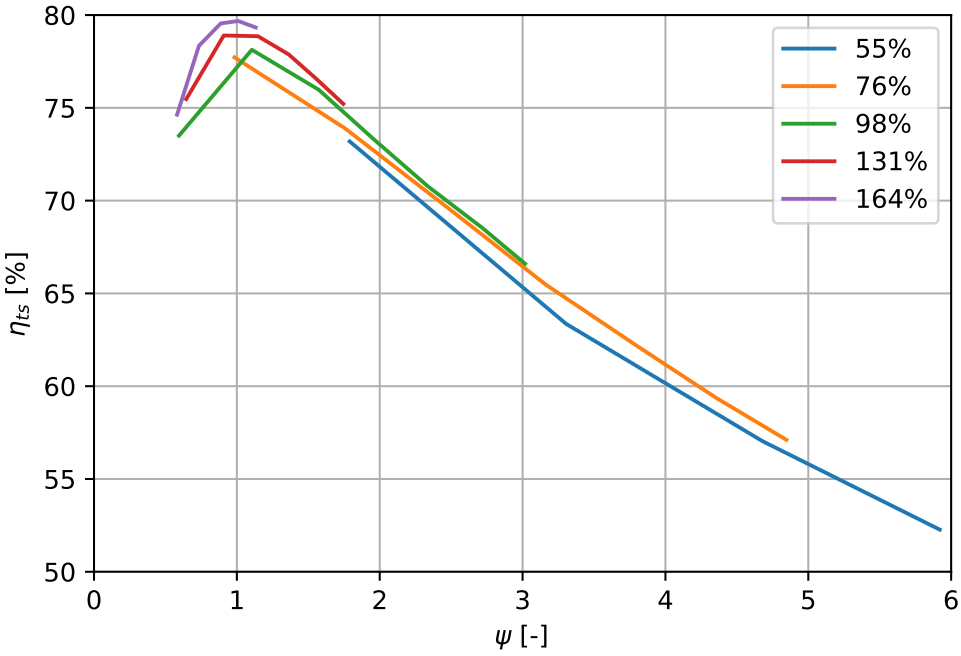

Figure 4.23.: Efficiency as a function of off design stage loading for differernt corrected speed, case B, TL. Calculated in MULTALL.

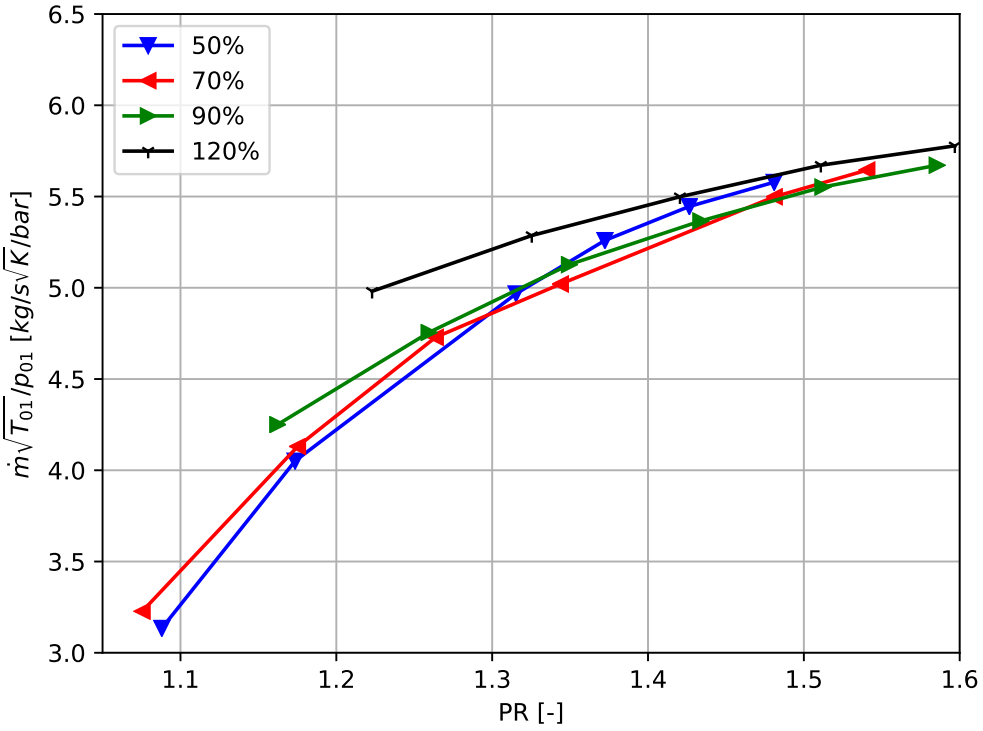

Figure 4.24.: Corrected mass flow for different correct speed as fraction of the design corrected speed, TH. Calculated in MULTALL.

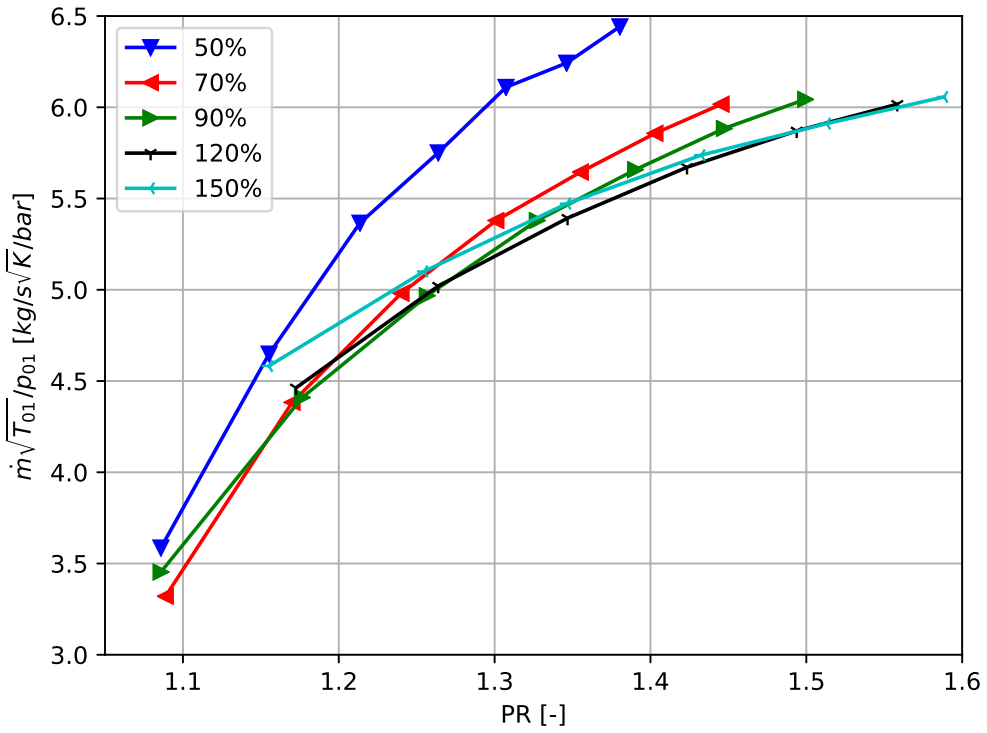

Figure 4.25.: Corrected mass flow for different correct speed as fraction of the design corrected speed, TL. Calculated in MULTALL.

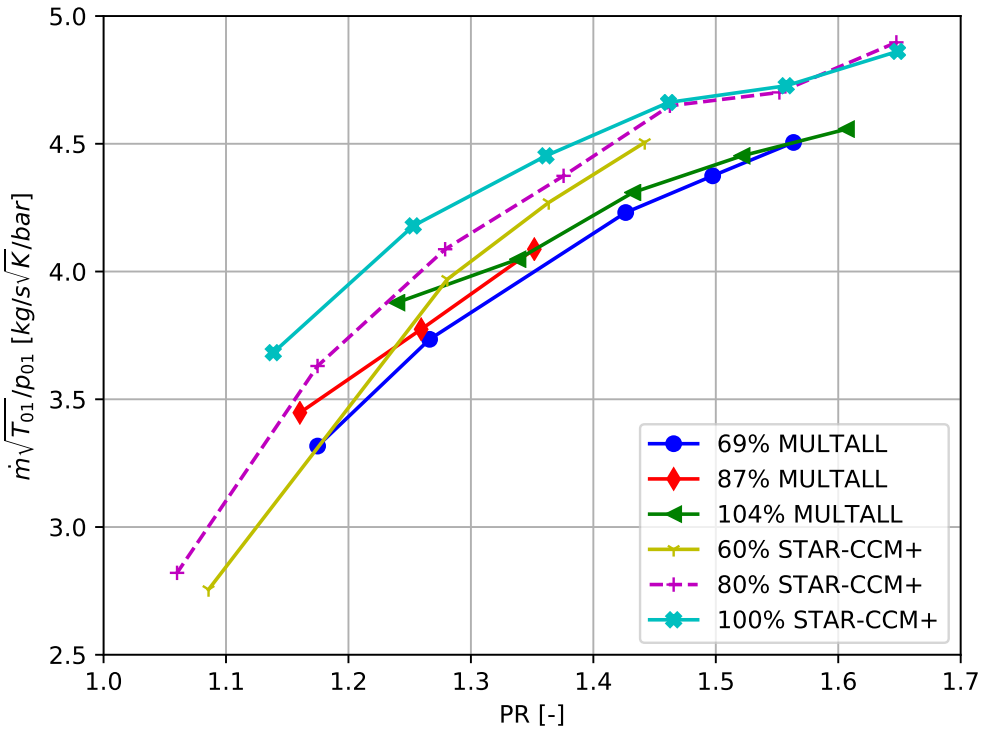

Figure 4.26.: Corrected mass flow for different correct speed as fraction of the design corrected speed. Calculated in MULTALL and STAR-CCM+ for a separate turbine

Chapter 5.

Conclusions

In this thesis a complete investigation of the Denton software package has been performed with good result and accuracy. The results has been validated to STAR-CCM+ as an accurate source. The software has been used to resemble a base turbine design with an efficiency difference less than 1%. The Denton software package did unfortunately not create a turbine with sufficient swallowing capacity when comparing to the base turbine design. The causes has been discussed and the plausible reasons come from the alterations in the source code made to mimic the base design. However this reduction in swallowing capacity occurred only when altering the source code for this particular case. Other turbines werre made without this problem. The computations for swallowing capacity made in MULTALL did not correspond to the result calculated in STAR-CCM+ with the result from MULTALL was smaller in corrected mass flow. The corrected mass flow calculated in MULTALL was approximately 6.3% for a pressure ratio of approximately 1.7.
The new configuration of an electric turbo compound will as noted by other literature and in this thesis greatly improve the overall efficiency of the turbo compound turbine. As the pressure ratio over the turbine increases, the efficiency is improved when increasing the corrected speed of the turbine. Two E-TC designs were designed, one designed with high rotational speed and one with low rotational speed, and they behaved similarly in the different flow cases. From the result shown in this thesis a E-TC designed for higher revolution speeds of 55 000 rpm should be more suitable as it operates closer to the design case throughout the overall operation.

With the work performed in this thesis, the author deems that Denton's software package is an easy to use first-hand design tool in turbine design for this particular application with a powerful CFD solver.

Bibliography

[1] C. of the European Union. (2019, Accessed 2020-05-05). "Cutting emissions: Council adopts co2 standards for trucks", [Online]. Available: https://www.consilium.europa.eu/sv/press/press-releases/2019/06/13/cutting-emissions-council-adopts-co2-standards-for-trucks/.

[2] S. L. Dixon and C Hall, *Fluid mechanics and thermodynamics of turbomachinery*. Butterworth-Heinemann, 2013.

[3] Y. A. Cengel and M. A. Boles, *Thermodynamics: an Engineering Approach, 8th edittion*. New York: McGraw-Hill Education, 2015.

[4] J. D. Anderson, "Fundamentals of aerodynamics", *NY: McGraw-Hill*, 2011.

[5] N. C. Baines, *Turbine Design and Analysis*. 2019.

[6] J. D. Denton, "The 1993 igti scholar lecture: Loss mechanisms in turbomachines", 1993.

[7] C. H. Sieverding, "Recent progress in the understanding of basic aspects of secondary flows in turbine blade passages", *J. Eng. Gas Turbines Power*, 1985.

[8] D. G. Ainley and G. C. Mathieson, "A method of performance estimation for axial-flow turbines", AERONAUTICAL RESEARCH COUNCIL LONDON (UNITED KINGDOM), Tech. Rep., 1951.

[9] H. I. H. Saravanamuttoo, G. F. C. Rogers and H Cohen, *Gas turbine theory*. Pearson Education, 2017.

[10] *Effects of Turbine Tip Clearance on Gas Turbine Performance*, 2008.

[11] P Lampart, "Tip leakage flows in turbines", *TASK QUARTERLY*, 2006.

[12] P Lampart, A. Gardzilewicz, A. V. Rusanov and S Yershov, "The effect of stator blade compound lean and compound twist on flow characteristics of a turbine stage - numerical study based on 3d ns simulations", *something*, 1999.

[13] H. K. Versteeg and W Malalasekera, *An introduction to computational fluid dynamics: the finite volume method*. Pearson education, 2007.

[14] W. P. (2019, Accessed 2020-05-05). "Napier nomad compound aircraft engine", [Online]. Available: https://oldmachinepress.com/2019/08/05/napier-nomad-compound-aircraft-engine/.

[15] Scania. (2001, Accessed 2020-05-08). "Scania produces 4 eco-point engine from oct 2001", [Online]. Available: https://web.archive.org/web/20110807165744/http://www.scania.com/%28S%28ebn3pnjrzi4q5wm4hwql15y5%29%29/media/pressreleases/2001070614en.aspx.

[16] G Pasini, G Lutzemberger, S Frigo, S Marelli, M Ceraolo, R Gentili and M Capobianco, "Evaluation of an electric turbo compound system for si engines: A numerical approach", *Applied Energy*, 2016.

[17] P Divekar, B Ayalew and R Prucka, "Coordinated electric supercharging and turbo-generation for a diesel engine", Apr. 2010. DOI: 10.4271/2010-01-1228.

[18] motorsport.com. (2011, Accessed 2020-05-05). "F1 set for electric only in the pit lane?", [Online]. Available: https://www.motorsport.com/f1/news/f1-set-for-electric-only-in-the-pit-lane/3218374/?utm_source=jaonf1.com&utm_medium=acquisition-redirect&utm_content=f1-set-for-electric-only-in-the-pit-lane.

[19] J. B. Heywood, *Combustion Engine Fundamentals*. McGraw-Hill, 1988.

[20] J. D. Denton, "Multall—an open source, computational fluid dynamics based, turbomachinery design system", *Journal of Turbomachinery*, 2017.

Appendix A.

Mesh

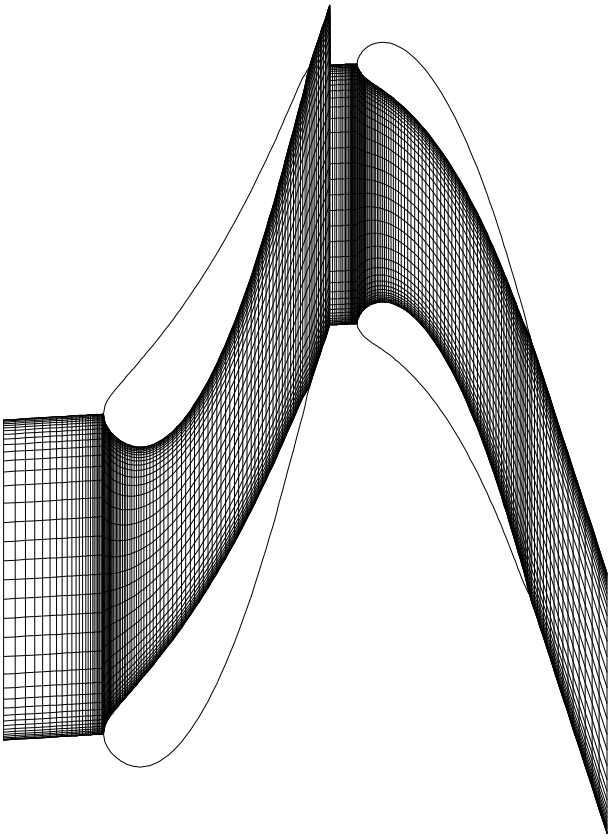

Figure A.1.: Mid section mesh for turbine TH, constructed through MULTALL

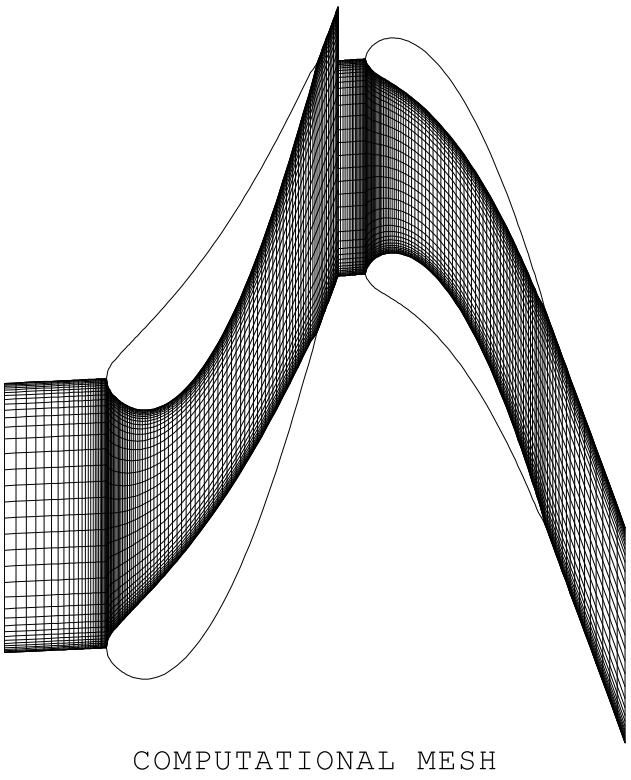

Figure A.2.: Mid section mesh for turbine TL, constructed through MULTALL

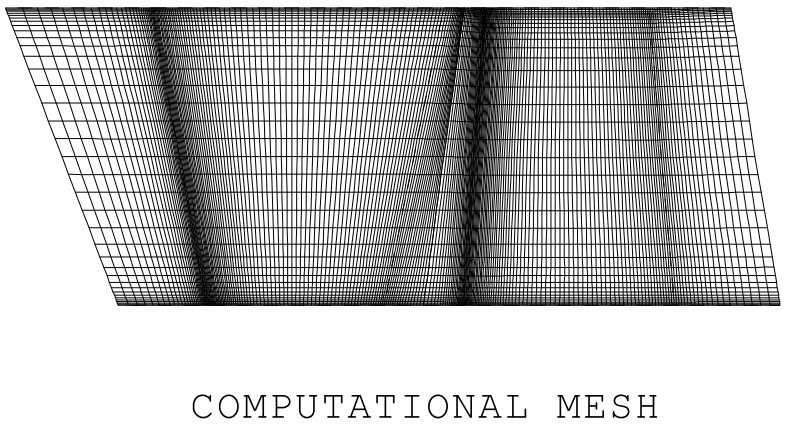

Figure A.3.: Meridional mesh for turbine TH, constructed through MULTALL

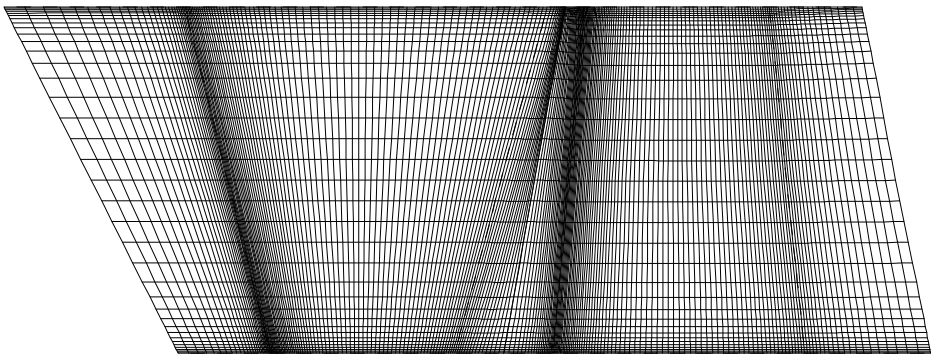

Figure A.4.: Meridional mesh for turbine TL, constructed through MULTALL

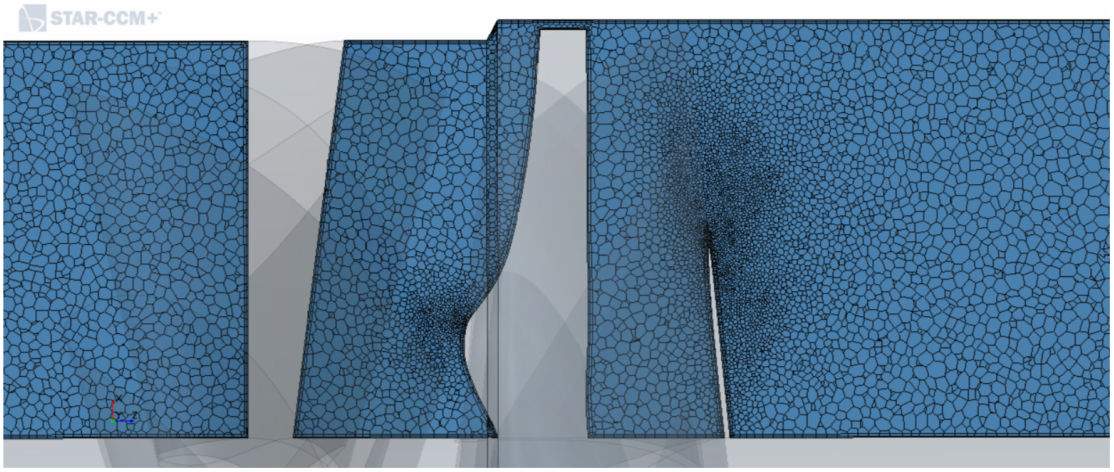

Figure A.5.: Meridional mesh for TL, constructed in STAR-CCM+

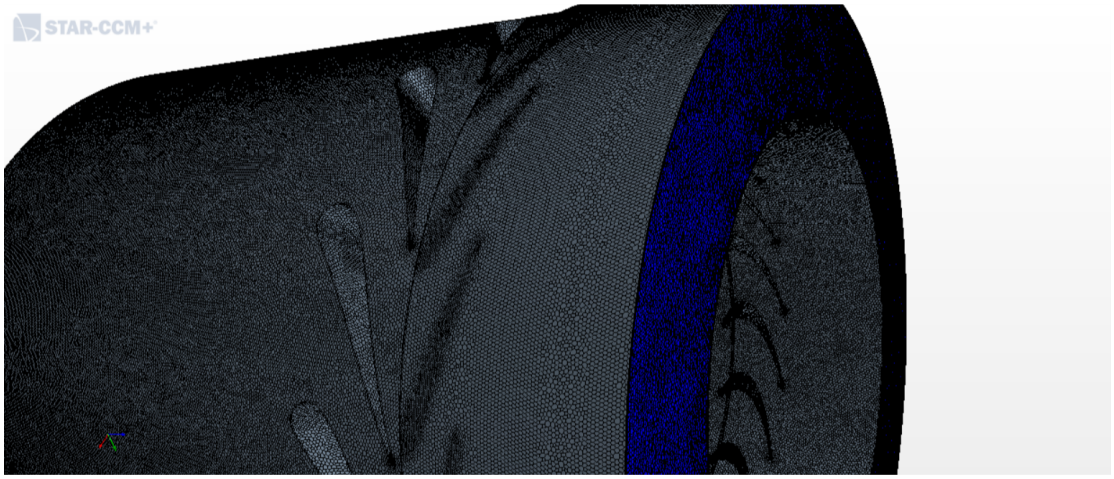

Figure A.6.: 3D view mesh for TL, constructed in STAR-CCM+

Appendix B.

CFD

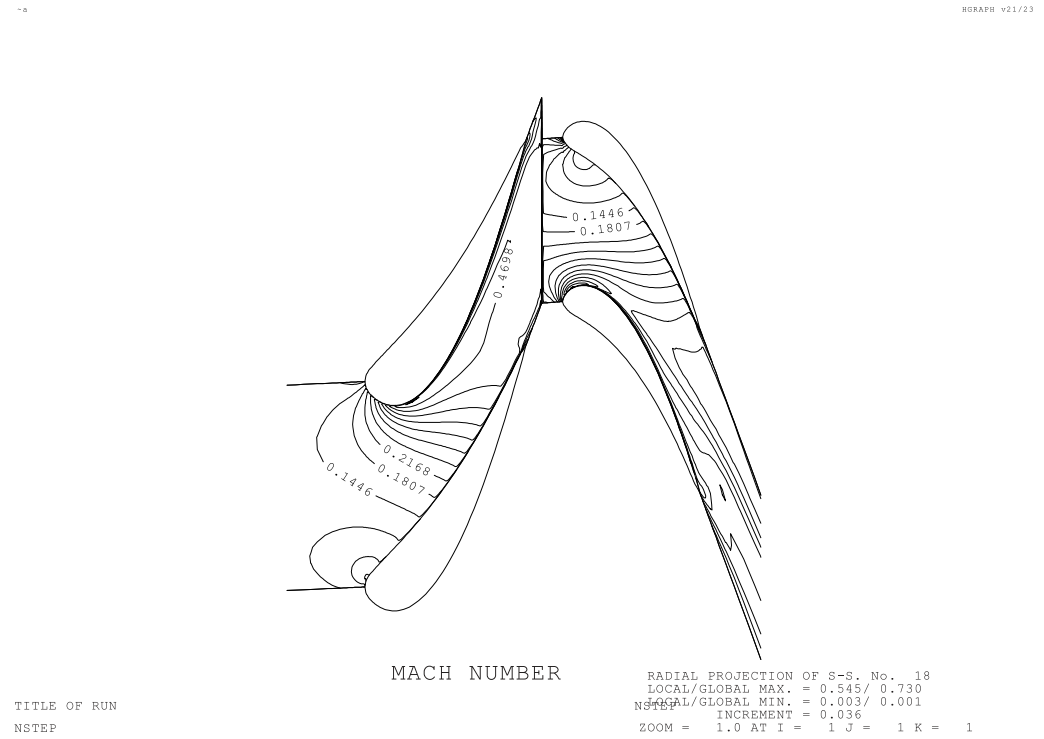

Figure B.1.: Contour plot for relative Mach number, mid section TL. Constructed through Multall

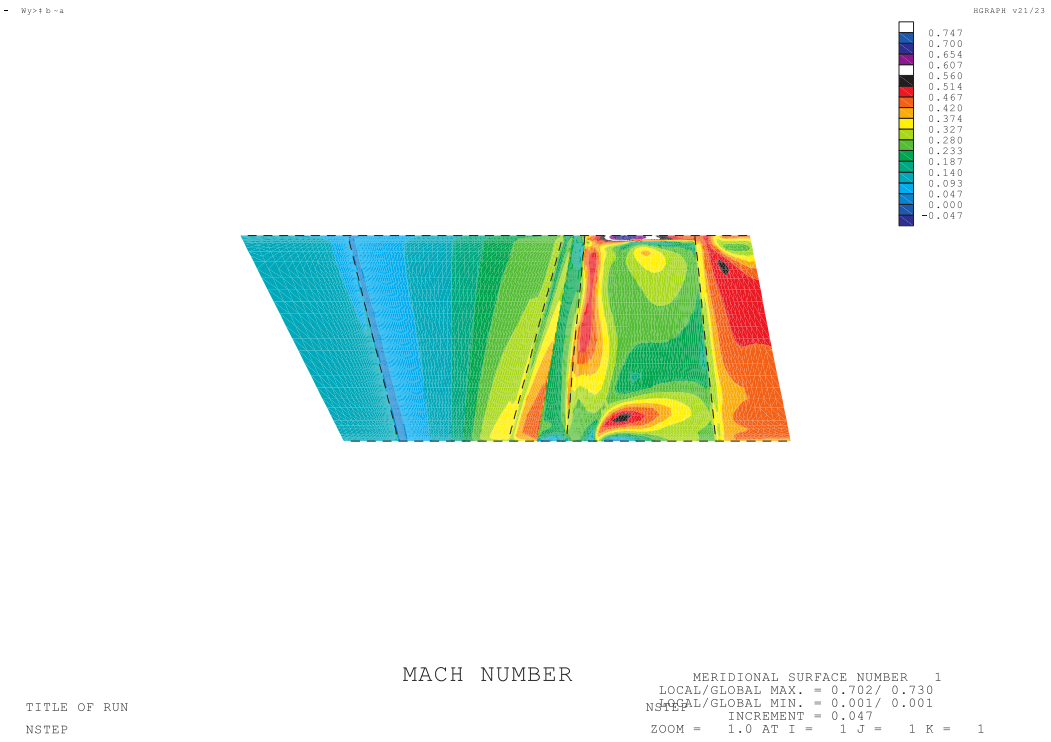

Figure B.2.: Contour plot for relative Mach number, meridional view TL. Constructed through Multall

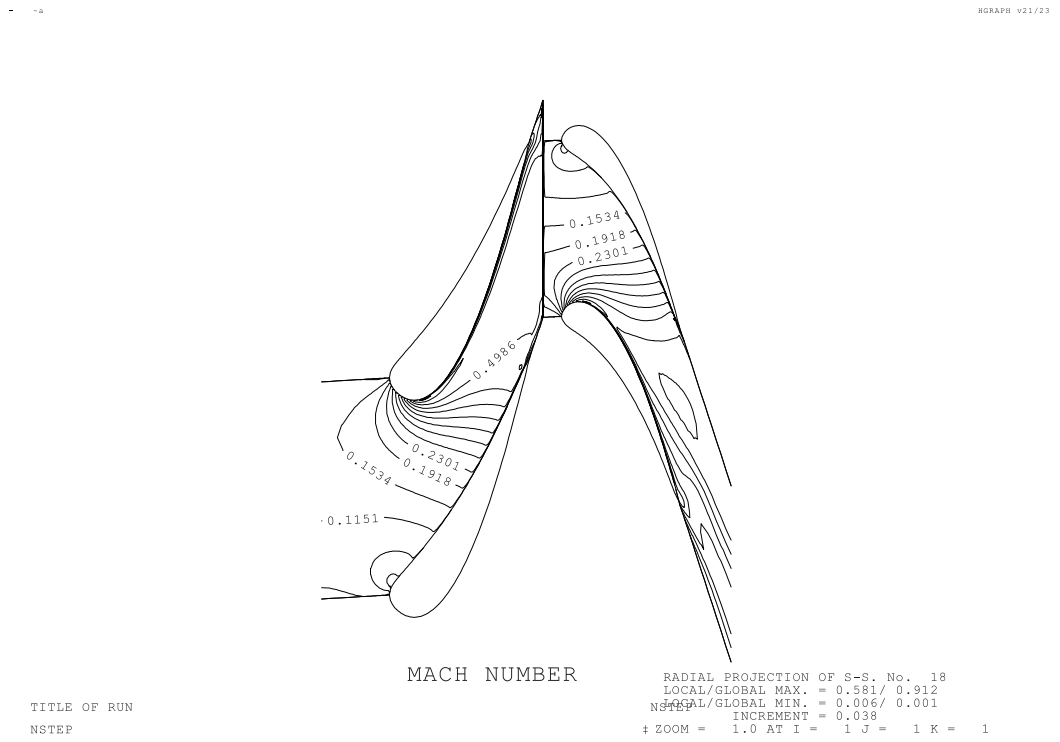

Figure B.3.: Contour plot for relative Mach number, mid section TH. Constructed through Multall

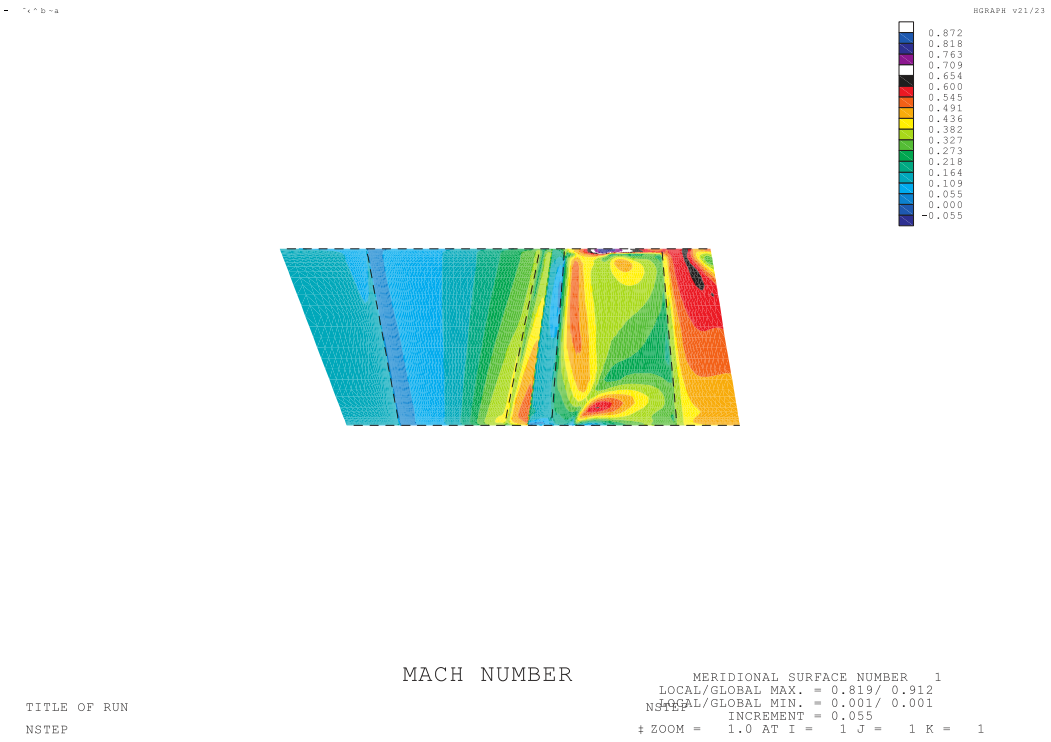

Figure B.4.: Contour plot for relative Mach number, meridional view TH. Constructed through Multall

Appendix C.

MEANGEN

```
T                       TURBO_TYP,"C" FOR A COMPRESSOR,"T" FOR A TURBINE
AXI                     FLO_TYP FOR AXIAL OR MIXED FLOW MACHINE
   287.500     1.3400     GAS PROPERTOES, RGAS, GAMMA
     2.100   778.000     POIN,  TOIN
    1                    NUMBER OF STAGES IN THE MACHINE
M                       CHOICE OF DESIGN POINT RADIUS, HUB, MID or TIP
   55000                ROTATION SPEED, RPM
       0.382            MASS FLOW RATE, FLOWIN.
D                       INTYPE, TO CHOOSE THE METHOD OF DEFINING THE VELOCITY TRIANGLES
  0.00  71 0.500        FIRST BLADE ROW ANGLES, REACTION
A                       RADTYPE, TO CHOOSE THE DESIGN POINT RADIUS
       0.0495           THE DESIGN POINT RADIUS
       0.015       0.012 BLADE AXIAL CHORDS IN METRES.
       0.250       0.500 ROW GAP  AND STAGE GAP
   0.00000   0.00000     BLOCKAGE FACTORS, FBLOCK_LE,  FBLOCK_TE
       0.900            GUESS OF THE STAGE ISENTROPIC EFFICIENCY
   2.000   2.000        ESTIMATE OF THE FIRST AND SECOND ROW DEVIATIONANGLES
  -2.000  -2.000        FIRST AND SECOND ROW INCIDENCE ANGLES
   1.00000              BLADE TWIST OPTION, FRAC_TWIST
N                       BLADE ROTATION OPTION , Y or N
 104.000  76.000        QO ANGLES AT LE  AND TE OF ROW 1
  85.000  95.000        QO ANGLES AT LE  AND TE OF ROW 2
N                       DO YOU WANT TO CHANGE THE ANGLES FOR THIS STAGE ? "Y" or "N"
Y                       IS OUTPUT REQUESTED FOR ALL BLADE ROWS ?
Y    STATOR No.  1 SET ANSTK = "Y" TO USE THE SAME BLADE SECTIONS AS THE LAST STAGE
Y    ROTOR No.   1 SET ANSTK = "Y" TO USE THE SAME  BLADE SECTIONS AS THE LAST STAGE
```

Figure C.1.: MEANGEN input data for turbine TH used in the report